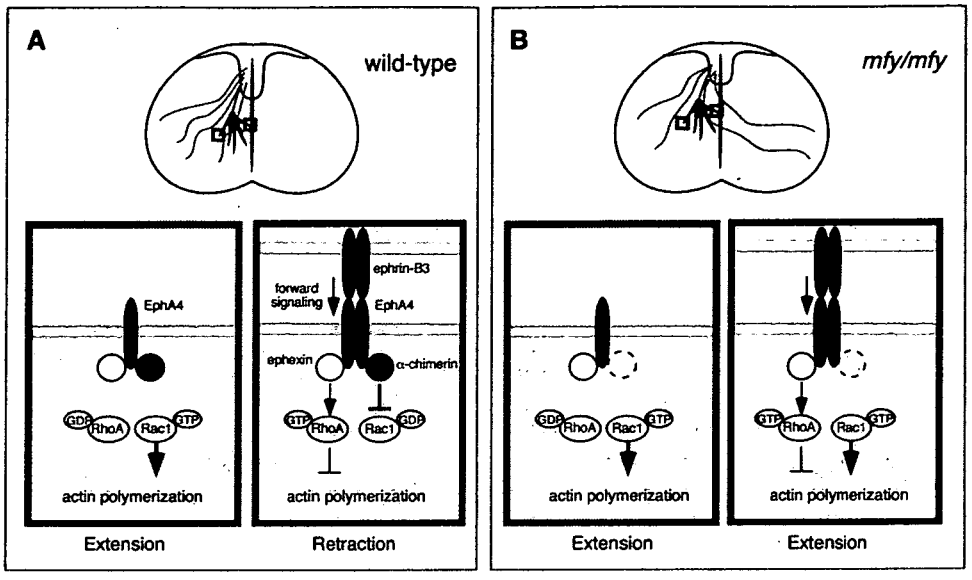

Figure 7. Model of EphrinB3/EphA4 Forward Signaling in Midline Repulsion of CST Axons

(A) In WT mice, the growth cones of CST axons extend due to basal activity of Rac, which is a positive regulator of process outgrowth, in the absence of ephrinB3 stimulation (green box). At the spinal cord midline that anchors ephrinB3, CST axons that express EphA4 receive forward signals. This ephrinB3/EphA4 forward signaling inactivates Rac through α-chimerin, leading to growth cone retraction (red box). Ephrin/EphA signaling might also activate RhoA, which is a negative regulator of process outgrowth, via ephexin (Shamah et al., 2001). The cooperative action of the RhoA-activator ephexin and the Rac-inactivator α-chimerin might induce efficient retraction of growth cones.

(B) In *mfy/mfy* mice, CST axons fail to stop at the midline due to the absence of α-chimerin-induced Rac inactivation, even in the presence of ephexin.

ephexin-induced RhoA activation. In contrast to the absence of an *Ephexin1* KO phenotype, we demonstrated that the formation of CST and CPGs is impaired in *α-Chn* mutant mice.

Critical Role of Rho-GTPase Inactivation in Ephrin/Eph Signaling

Ephrin/Eph signaling is important in a wide range of biological processes, including oocyte maturation, early morphogenesis, segmentation, guidance of migrating cells, synaptic plasticity, dendritic-spine formation, and axon guidance (Flanagan and Vanderhaeghen, 1998; Palmer and Klein, 2003; Pasquale, 2005). Recent studies of in vitro orientation suggest that in various biological phenomena, ephrin/Eph signaling regulates actin dynamics by activating Rho-GTPases, such as RhoA, Rac, and Cdc42, through Rho-GEFs (Cowan et al., 2005; Fu et al., 2007; Irie and Yamaguchi, 2002; Murai and Pasquale, 2005; Ogita et al., 2003; Penzes et al., 2003; Shamah et al., 2001; Tanaka et al., 2004). We suggest that a further mode of ephrin/Eph signaling exists, in which Ephs regulate actin dynamics by inactivating Rho-GTPases through Rho-GAPs.

Ephrin/Eph signaling might control actin dynamics by regulating the balance between negative regulators of actin polymerization (such as RhoA) and positive regulators (such as Rac and Cdc42; Sahin et al., 2005; Shamah et al., 2001). This theory only takes into account Rho-activation; however, we have now shown that Rho-inactivation is another important aspect of the ephrin/Eph regulation of actin dynamics. The activity of each Rho-GTPase might be controlled by the balance between its activation by Rho-GEFs and its inactivation by Rho-GAPs. In mammalian cells, there are many diverse Rho-GEFs and Rho-GAPs with different substrate specificities that are controlled by different mechanisms (Etienne-Manneville and Hall, 2002). Thus, it is possible that ephrin/Eph signaling in different processes employs specific Rho-GEFs and/or Rho-GAPs to achieve the appropriate balance of activity of each Rho-GTPase. In short, we propose that ephrin/Eph signaling regulates actin dynamics in two ways: first, by regulating the balance between the activities of different Rho-GTPases (such as RhoA and Rac or Cdc42), and second, by regulating the balance between activation and inactivation of each individual Rho-GTPase.

Regulation and Roles of α-Chimerin in Neural Development and Function

The present study provides evidence for the involvement of α-chimerin in ephrinB3/EphA4 forward signaling. How does ephrinB3/EphA4 signaling activate α-chimerin? As the kinase-inactive EphA4^{FF} mutant protein could not activate α-chimerin (Figure 5F), it appeared that the kinase activity of EphA4 was necessary for the activation of α-chimerin. However, EphA4 kinase activity alone did not appear to be sufficient as the EphA4 proteins overexpressed in COS cells were phosphorylated and, thus,

kinase active, but were unable to fully activate α-chimerin in the absence of ephrinB3 stimulation (Figures 5E and 5F). In fact, it has been shown that the kinase activity of EphA4 alone is not sufficient for ephrinB/EphA4 forward signaling in vivo: the *EphA4*$^{EE/EE}$ mouse, the kinase of which is constitutively activated, has a normal alternate gait, normal CST axon midline guidance, normal CPG midline guidance, and normal morphology of the spinal cord (Egea et al., 2005). Cultured cortical neurons derived from *EphA4*$^{EE/EE}$ mice undergo normal growth cone collapse in response to clustered ephrinB3. Based on these observations, it has been proposed that higher-order clustering of EphA4 by stimulation of ephrinB is an essential component of ephrinB/EphA4 forward signaling (Egea et al., 2005). Our results are consistent with this idea.

Both the α1 and α2 isoforms of α-chimerin have a single copy of the C1 domain, which is a cysteine-rich motif, and can be activated by the binding of phorbol esters or diacylglycerol (DAG) to the C1 domain (Hall et al., 1990, 1993). Recently, it was reported that cyclin-dependent kinase 5 (Cdk5) regulates EphA4-mediated dendritic-spine retraction (Fu et al., 2007). Cdk5 is known to interact with α2-chimerin (Qi et al., 2004), so it is possible that a protein complex formed by clustering of EphA4 recruits some additional molecules required for linking activated EphA4 to α-chimerin activation. Such additional factors could include Cdk5/p35 and DAG-producing enzymes, such as phospholipase Cγ. It should be noted that these (or equivalent) factors do not appear to be specific to neurons, but rather are ubiquitous, as the expression of EphA4 and α2 isoforms in COS cells was sufficient to inactivate Rac upon stimulation by clustered-ephrinB3 (Figures 5E and 5F).

The *α-Chn* gene is widely expressed in the central nervous system both during development and in adulthood (Hall et al., 2001, 1990, 1993), and α-chimerin is found not only in axons but also in neuronal dendrites (Hall et al., 2001). It would be interesting to test whether α-chimerin plays a role in dendrite development in the brain. Recent studies using overexpression and/or siRNA-induced knockdown of α1-chimerin in cultured hippocampal neurons and cerebellar slices suggest that it regulates dendritic morphology and dendritic-spine density (Buttery et al., 2006; Van de Ven et al., 2005). α-chimerin might also be involved in NMDA receptor-dependent developmental plasticity, such as maturation of the barrel cortex (Iwasato et al., 2000, 1997), as well as in learning and memory, as it has been shown to interact with NMDA receptors in vitro (Van de Ven et al., 2005). The *mfy/mfy* mouse is thus a promising experimental model for elucidating the roles of α-chimerin Rac-GAP in the development and function of the central nervous system.

EXPERIMENTAL PROCEDURES

Animals

A Tg construct was made by modifying the RP23-413N9 BAC clone derived from B6 mouse genomic DNA (Roswell Park Cancer Institute, NY, USA). The Tg founder mice were generated by microinjection of linearized constructs into fertilized eggs. *α-Chn* KO mice were generated using MS12 ES cells derived from the B6 strain (for details see the Supplemental Experimental Procedures). All of the mice were maintained according to the institutional guidelines of the animal facilities of the RIKEN-BSI.

VR Recordings

P1–P3 mice were anesthetized with isoflurane, and their spinal cords were removed as described elsewhere (Nishimaru et al., 2006). Electrical recordings of the VRs were made with glass-suction electrodes, and locomotor-like rhythmic activity was evoked by the concomitant bath application of NMDA (4–7 μM) and serotonin (5HT; 4–7 μM). Details of the recording procedure and data analyses are provided in the Supplemental Data.

Linkage Analyses

PCR primers for the microsatellite markers and SNPs were designed using the Mouse Genome Informatics (http://www.informatics.jax.org/) and National Centre for Biotechnology Information (http://www.ncbi.nlm.nih.gov/SNP/) databases, respectively, and were verified by PCR using the genomic DNAs of inbred B6 and DBA/2 mice and B6/DBA F_1 hybrids (for detailed methods, see Figure S3 and Supplemental Data).

Generation of Antibody

KLH-coupled synthetic peptides (MALTLFDTDEYRPPVWKC) corresponding to the N terminus of α2-chimerin (Figure S4A) were used to raise a rabbit polyclonal antibody (BSI Research Resources Center). Sera were affinity purified on the same peptides.

Measurement of Rac1 Activity

Transfected COS-7 cells were stimulated with 2 μg/ml preclustered ephrinB3-Fc (R&D Systems) in serum-free medium for 10 min. The cells were lysed with ice-cold cell lysis buffer containing 4 μg of GST-CRIB of αPak (amino acids 70–150). After centrifugation, the supernatant was incubated with glutathione-Sepharose beads, and bound proteins were analyzed by SDS-PAGE and immunoblotting (for detailed methods, see Supplemental Data).

Growth Cone Collapse Assay

Primary neurons were dissociated from the anterior dorsomedial to dorsal neocortex of E16.5 mice or E18.5 rats as described elsewhere (Ishikawa et al., 2003, Kullander et al., 2001a). The neurons were plated onto poly-D-lysine and laminin-coated coverslips and cultured in Neurobasal medium supplemented with 2% B27 (Invitrogen). They were then stimulated with 5 μg/ml preclustered ephrinB3-Fc for 30 min, fixed with 4% paraformaldehyde, and stained with rhodamine-conjugated phalloidin (Invitrogen; for detailed methods, see Supplemental Data).

Supplemental Data

Supplemental Data include Experimental Procedures, References, nine figures, and one table and can be found with this article online at http://www.cell.com/cgi/content/full/130/4/742/DC1/.

ACKNOWLEDGMENTS

We thank N. Ichinohe, S. Nishimura, Y. Sano, M. Tanaka, J. S. Park, and M. Fujita for advice on the experiments; T. Koganezawa for help with the analysis of electrophysiological data; T. Usami and H. Suzuki for technical assistance; H. Nishiyama for comments on the manuscript; the BSI Research Resources Center for animal care and technical assistance; J. Miyazaki and T. Saito for the CAG-EYFP vector; and K. Yaguchi for the pCR-FRT-amp-FRT plasmid. This work was supported, in part, by PRESTO, JST (to T.I.) and by a Grant-in-Aid for

Scientific Research on Priority Areas from the MEXT, Japan (to T.I. and H.K.).

Received: February 20, 2007
Revised: May 24, 2007
Accepted: July 16, 2007
Published: August 23, 2007

REFERENCES

Ahmed, S., Lee, J., Wen, L.P., Zhao, Z., Ho, J., Best, A., Kozma, R., and Lim, L. (1994). Breakpoint cluster region gene product-related domain of n-chimaerin. Discrimination between Rac-binding and GTPase-activating residues by mutational analysis. J. Biol. Chem. *269*, 17642–17648.

Brown, M., Jacobs, T., Eickholt, B., Ferrari, G., Teo, M., Monfries, C., Qi, R.Z., Leung, T., Lim, L., and Hall, C. (2004). Alpha2-chimaerin, cyclin-dependent kinase 5/p35, and its target collapsin response mediator protein-2 are essential components in semaphorin 3A-induced growth-cone collapse. J. Neurosci. *24*, 8994–9004.

Buttery, P., Beg, A.A., Chih, B., Broder, A., Mason, C.A., and Scheiffele, P. (2006). The diacylglycerol-binding protein alpha1-chimaerin regulates dendritic morphology. Proc. Natl. Acad. Sci. USA *103*, 1924–1929.

Cowan, C.W., Shao, Y.R., Sahin, M., Shamah, S.M., Lin, M.Z., Greer, P.L., Gao, S., Griffith, E.C., Brugge, J.S., and Greenberg, M.E. (2005). Vav family GEFs link activated Ephs to endocytosis and axon guidance. Neuron *46*, 205–217.

Diekmann, D., Brill, S., Garrett, M.D., Totty, N., Hsuan, J., Monfries, C., Hall, C., Lim, L., and Hall, A. (1991). Bcr encodes a GTPase-activating protein for p21rac. Nature *351*, 400–402.

Dottori, M., Hartley, L., Galea, M., Paxinos, G., Polizzotto, M., Kilpatrick, T., Bartlett, P.F., Murphy, M., Kontgen, F., and Boyd, A.W. (1998). EphA4 (Sek1) receptor tyrosine kinase is required for the development of the corticospinal tract. Proc. Natl. Acad. Sci. USA *95*, 13248–13253.

Egea, J., Nissen, U.V., Dufour, A., Sahin, M., Greer, P., Kullander, K., Mrsic-Flogel, T.D., Greenberg, M.E., Kiehn, O., Vanderhaeghen, P., et al. (2005). Regulation of EphA 4 kinase activity is required for a subset of axon guidance decisions suggesting a key role for receptor clustering in Eph function. Neuron *47*, 515–528.

Eph Nomenclature Committee (1997). Unified nomenclature for Eph family receptors and their ligands, the ephrins. Cell *90*, 403–404.

Etienne-Manneville, S., and Hall, A. (2002). Rho GTPases in cell biology. Nature *420*, 629–635.

Flanagan, J.G., and Vanderhaeghen, P. (1998). The ephrins and Eph receptors in neural development. Annu. Rev. Neurosci. *21*, 309–345.

Fu, W.Y., Chen, Y., Sahin, M., Zhao, X.S., Shi, L., Bikoff, J.B., Lai, K.O., Yung, W.H., Fu, A.K., Greenberg, M.E., et al. (2007). Cdk5 regulates EphA4-mediated dendritic spine retraction through an ephexin1-dependent mechanism. Nat. Neurosci. *10*, 67–76.

Gianino, S., Stein, S.A., Li, H., Lu, X., Biesiada, E., Ulas, J., and Xu, X.M. (1999). Postnatal growth of corticospinal axons in the spinal cord of developing mice. Brain Res. Dev. Brain Res. *112*, 189–204.

Grillner, S., and Wallen, P. (1985). Central pattern generators for locomotion, with special reference to vertebrates. Annu. Rev. Neurosci. *8*, 233–261.

Hall, C., Monfries, C., Smith, P., Lim, H.H., Kozma, R., Ahmed, S., Vanniasingham, V., Leung, T., and Lim, L. (1990). Novel human brain cDNA encoding a 34,000 Mr protein n-chimaerin, related to both the regulatory domain of protein kinase C and BCR, the product of the breakpoint cluster region gene. J. Mol. Biol. *211*, 11–16.

Hall, C., Sin, W.C., Teo, M., Michael, G.J., Smith, P., Dong, J.M., Lim, H.H., Manser, E., Spurr, N.K., Jones, T.A., et al. (1993). Alpha 2-chimerin, an SH2-containing GTPase-activating protein for the ras-related protein p21rac derived by alternate splicing of the human n-chimerin gene, is selectively expressed in brain regions and testes. Mol. Cell. Biol. *13*, 4986–4998.

Hall, C., Michael, G.J., Cann, N., Ferrari, G., Teo, M., Jacobs, T., Monfries, C., and Lim, L. (2001). Alpha2-chimaerin, a Cdc42/Rac1 regulator, is selectively expressed in the rat embryonic nervous system and is involved in neuritogenesis in N1E–115 neuroblastoma cells. J. Neurosci. *21*, 5191–5202.

Inoue, H., Tsukita, K., Iwasato, T., Suzuki, Y., Tomioka, M., Tateno, M., Nagao, M., Kawata, A., Saido, T.C., Miura, M., et al. (2003). The crucial role of caspase-9 in the disease progression of a transgenic ALS mouse model. EMBO J. *22*, 6665–6674.

Irie, F., and Yamaguchi, Y. (2002). EphB receptors regulate dendritic spine development via intersectin, Cdc42 and N-WASP. Nat. Neurosci. *5*, 1117–1118.

Ishikawa, Y., Katoh, H., and Negishi, M. (2003). A role of Rnd1 GTPase in dendritic spine formation in hippocampal neurons. J. Neurosci. *23*, 11065–11072.

Iwasato, T., Erzurumlu, R.S., Huerta, P.T., Chen, D.F., Sasaoka, T., Ulupinar, E., and Tonegawa, S. (1997). NMDA receptor-dependent refinement of somatotopic maps. Neuron *19*, 1201–1210.

Iwasato, T., Datwani, A., Wolf, A.M., Nishiyama, H., Taguchi, Y., Tonegawa, S., Knopfel, T., Erzurumlu, R.S., and Itohara, S. (2000). Cortex-restricted disruption of NMDAR1 impairs neuronal patterns in the barrel cortex. Nature *406*, 726–731.

Kiehn, O., and Kullander, K. (2004). Central pattern generators deciphered by molecular genetics. Neuron *41*, 317–321.

Kullander, K., Croll, S.D., Zimmer, M., Pan, L., McClain, J., Hughes, V., Zabski, S., DeChiara, T.M., Klein, R., Yancopoulos, G.D., et al. (2001a). Ephrin-B3 is the midline barrier that prevents corticospinal tract axons from recrossing, allowing for unilateral motor control. Genes Dev. *15*, 877–888.

Kullander, K., Mather, N.K., Diella, F., Dottori, M., Boyd, A.W., and Klein, R. (2001b). Kinase-dependent and kinase-independent functions of EphA4 receptors in major axon tract formation *in vivo*. Neuron *29*, 73–84.

Kullander, K., Butt, S.J., Lebret, J.M., Lundfald, L., Restrepo, C.E., Rydstrom, A., Klein, R., and Kiehn, O. (2003). Role of EphA4 and EphrinB3 in local neuronal circuits that control walking. Science *299*, 1889–1892.

Liang, F.Y., Moret, V., Wiesendanger, M., and Rouiller, E.M. (1991). Corticomotoneuronal connections in the rat: evidence from double-labeling of motoneurons and corticospinal axon arborizations. J. Comp. Neurol. *311*, 356–366.

Luo, L. (2000). Rho GTPases in neuronal morphogenesis. Nat. Rev. Neurosci. *1*, 173–180.

Murai, K.K., and Pasquale, E.B. (2005). New exchanges in eph-dependent growth cone dynamics. Neuron *46*, 161–163.

Nishimaru, H., and Kudo, N. (2000). Formation of the central pattern generator for locomotion in the rat and mouse. Brain Res. Bull. *53*, 661–669.

Nishimaru, H., Restrepo, C.E., and Kiehn, O. (2006). Activity of Renshaw cells during locomotor-like rhythmic activity in the isolated spinal cord of neonatal mice. J. Neurosci. *26*, 5320–5328.

Noren, N.K., and Pasquale, E.B. (2004). Eph receptor-ephrin bidirectional signals that target Ras and Rho proteins. Cell. Signal. *16*, 655–666.

Ogita, H., Kunimoto, S., Kamioka, Y., Sawa, H., Masuda, M., and Mochizuki, N. (2003). EphA4-mediated Rho activation via Vsm-RhoGEF expressed specifically in vascular smooth muscle cells. Circ. Res. *93*, 23–31.

Palmer, A., and Klein, R. (2003). Multiple roles of ephrins in morphogenesis, neuronal networking, and brain function. Genes Dev. *17*, 1429–1450.

Pasquale, E.B. (2005). Eph receptor signalling casts a wide net on cell behaviour. Nat. Rev. Mol. Cell Biol. *6*, 462–475.

Penzes, P., Beeser, A., Chernoff, J., Schiller, M.R., Eipper, B.A., Mains, R.E., and Huganir, R.L. (2003). Rapid induction of dendritic spine morphogenesis by trans-synaptic ephrinB-EphB receptor activation of the Rho-GEF kalirin. Neuron *37*, 263–274.

Qi, R.Z., Ching, Y.P., Kung, H.F., and Wang, J.H. (2004). Alpha-chimerin exists in a functional complex with the Cdk5 kinase in brain. FEBS Lett. *561*, 177–180.

Sahin, M., Greer, P.L., Lin, M.Z., Poucher, H., Eberhart, J., Schmidt, S., Wright, T.M., Shamah, S.M., O'Connell, S., Cowan, C.W., et al. (2005). Eph-dependent tyrosine phosphorylation of ephexin1 modulates growth cone collapse. Neuron *46*, 191–204.

Shamah, S.M., Lin, M.Z., Goldberg, J.L., Estrach, S., Sahin, M., Hu, L., Bazalakova, M., Neve, R.L., Corfas, G., Debant, A., et al. (2001). EphA receptors regulate growth cone dynamics through the novel guanine nucleotide exchange factor ephexin. Cell *105*, 233–244.

Tanaka, M., Ohashi, R., Nakamura, R., Shinmura, K., Kamo, T., Sakai, R., and Sugimura, H. (2004). Tiam1 mediates neurite outgrowth induced by ephrin-B1 and EphA2. EMBO J. *23*, 1075–1088.

Van de Ven, T.J., VanDongen, H.M., and VanDongen, A.M. (2005). The nonkinase phorbol ester receptor alpha1-chimerin binds the NMDA receptor NR2A subunit and regulates dendritic spine density. J. Neurosci. *25*, 9488–9496.

Wahl, S., Barth, H., Ciossek, T., Aktories, K., and Mueller, B.K. (2000). Ephrin-A5 induces collapse of growth cones by activating Rho and Rho kinase. J. Cell Biol. *149*, 263–270.

Whelan, P., Bonnot, A., and O'Donovan, M.J. (2000). Properties of rhythmic activity generated by the isolated spinal cord of the neonatal mouse. J. Neurophysiol. *84*, 2821–2833.

Yokoyama, N., Romero, M.I., Cowan, C.A., Galvan, P., Helmbacher, F., Charnay, P., Parada, L.F., and Henkemeyer, M. (2001). Forward signaling mediated by ephrin-B3 prevents contralateral corticospinal axons from recrossing the spinal cord midline. Neuron *29*, 85–97.

Accession Numbers

The DNA sequences have been deposited in the DNA Data Bank of Japan (DDBJ) under the following accession numbers: AB264771 ($\alpha 1$-Chn^{mfy} cDNA), AB264772 ($\alpha 2$-Chn^{mfy} cDNA), AB264773 ($\alpha 3$-Chn^{mfy} cDNA), AB264774 ($\alpha 3$-Chn^{WT} cDNA), and AB264775 (retroposon).

Available online at www.sciencedirect.com
ScienceDirect
Neuroscience Research 59 (2007) 413–425
Neuroscience Research
www.elsevier.com/locate/neures

Pael receptor is involved in dopamine metabolism in the nigrostriatal system

Yuzuru Imai [a,1,*], Haruhisa Inoue [a,1,2], Ayane Kataoka [a], Wang Hua-Qin [a,2], Masao Masuda [c], Toshio Ikeda [b], Kayoko Tsukita [a], Mariko Soda [a], Tohru Kodama [d], Tatsu Fuwa [e], Yoshiko Honda [d], Satoshi Kaneko [f], Sadayuki Matsumoto [f], Kazumasa Wakamatsu [g], Shosuke Ito [g], Masami Miura [c], Toshihiko Aosaki [c], Shigeyoshi Itohara [b], Ryosuke Takahashi [a,**]

[a] *Laboratory for Motor System Neurodegeneration, RIKEN Brain Science Institute (BSI), Saitama 351-0198, Japan*
[b] *Laboratory for Behavioral Genetics, RIKEN Brain Science Institute (BSI), Saitama 351-0198, Japan*
[c] *Neural Circuits Dynamics Research Group, Tokyo Metropolitan Institute of Gerontology, Tokyo 173-0015, Japan*
[d] *Department of Psychology, Tokyo Metropolitan Institute for Neuroscience, Tokyo 183-8526, Japan*
[e] *Department of Neurology, Tokyo Metropolitan Institute for Neuroscience, Tokyo 183-8526, Japan*
[f] *Department of Neurology, Kitano Hospital, The Tazuke Kofukai Medical Research Institute, Osaka 530-8480, Japan*
[g] *Department of Chemistry, Fujita Health University School of Health Sciences, Aichi 470-1192, Japan*

Received 13 July 2007; accepted 10 August 2007
Available online 15 August 2007

Abstract

Pael receptor (Pael-R) has been identified as one of the substrates of Parkin, a ubiquitin ligase responsible for autosomal recessive juvenile Parkinsonism (AR-JP). When Parkin is inactivated, unfolded Pael-R accumulates in the endoplasmic reticulum and results in neuronal death by unfolded protein stress, suggesting that Pael-R has an important role in the pathogenesis of AR-JP. Here we report the analyses on Pael-R-deficient (KO) and Pael-R-transgenic (Tg) mice. The striatal dopamine (DA) level of Pael-R KO mice was only 60% of that in normal mice, while in Pael-R Tg mice, striatal 3,4-dihydroxyphenylacetic acid (DOPAC) as well as vesicular DA content increased. Moreover, the nigrostriatal dopaminergic neurons of Pael-R Tg mice are more vulnerable to Parkinson's disease-related neurotoxins while those of Pael-R KO mice are less. These results strongly suggest that the Pael-R signal regulates the amount of DA in the dopaminergic neurons and that excessive Pael-R expression renders dopaminergic neurons susceptible to chronic DA toxicity.

Keywords: Parkinson's disease; Parkin; Striatum; Substantia nigra; AR-JP; GPR37; MPTP; 6-OHDA

1. Introduction

DA is one of the important neurotransmitters of the central nervous system (CNS). Animal studies reveal that increasing synaptic DA concentration by inhibiting DA transporters or blocking DA autoreceptors stimulates locomotion and exploratory behavior. Conversely, blocking DA receptors attenuates the effects of food rewards, intracranial self-stimulation, and psychomotor stimulants. DA-deficient animals show severe adipsia, aphagia, hypoactivity, and impaired complicated motor behaviors (Zhou and Palmiter, 1995). About 75% of the dopaminergic neurons in the brain have their cell bodies in the substantia nigra (SN) of the basal ganglia and project to

* Corresponding author. Present address: Institute of Development, Aging and Cancer, Tohoku University, Sendai 980-8575, Japan. Tel.: +81 22 717 8490; fax: +81 22 717 8490.
** Corresponding author. Present address: Department of Neurology, Kyoto University School of Medicine, Kyoto 606-8507, Japan. Tel.: +81 75 751 3770; fax: +81 75 761 9780.
E-mail addresses: yimai@idac.tohoku.ac.jp (Y. Imai), ryosuket@kuhp.kyoto-u.ac.jp (R. Takahashi).
[1] These authors contributed equally to this work.
[2] Present address: Department of Neurology, Kyoto University School of Medicine, Kyoto 606-8507, Japan.

0168-0102/$ – see front matter
doi:10.1016/j.neures.2007.08.005

the striatum. Progressive loss of this population underlies Parkinson's disease (PD) in humans (Betarbet et al., 2002). Most cases of PD are sporadic and the etiology of common PD remains unknown. However, recent identification of gene mutations in familial cases of PD has advanced our understanding of the molecular mechanisms behind the neurodegeneration associated with this disease.

A major cause of juvenile PD, autosomal recessive juvenile Parkinsonism (AR-JP), results from mutations in the Parkin gene (Kitada et al., 1998). Parkin protein is a RING-finger type ubiquitin ligase (E3) and AR-JP-linked Parkin mutants are defective in E3 activity (Imai et al., 2000; Shimura et al., 2000; Zhang et al., 2000). The accumulation of unfolded Pael-R, a substrate for Parkin recently identified in our laboratory, causes unfolded protein stress, which results in cell death *in vivo* and *in vitro* (Imai et al., 2001; Yang et al., 2003). Parkin eliminates unfolded Pael-R in cooperation with the molecular chaperone Hsp70 and a U box protein known as CHIP (Imai et al., 2002). Pael-R, which is abundantly expressed in dopaminergic neurons of the SN, other regions (such as the hippocampus), and some nuclei of the brainstem and in oligodendrocytes, is a putative G protein coupled receptor whose ligand is unknown (Donohue et al., 1998; Imai et al., 2001) and whose physiological function in the brain remains unclear.

Here we provide genetic evidence in mice that Pael-R is involved in the regulation of nigrostriatal dopamine metabolism and propose a hypothesis of DA neuron-specific pathological mechanism by Pael-R expression.

2. Materials and methods

2.1. Targeted disruption of the mouse Pael-R gene

Pael-R KO mouse was generated by standard technique of gene targeting (Gomi et al., 1995). A targeting vector was constructed using 17.5-kb genomic DNA fragments containing exon 1 of Pael-R gene (Fig. 1C). Floxed pgk-neo cassette and loxP sequence were inserted at the sites of the intron 1 and untranslated region of exon 1, respectively. DT-ApA cassette was flanked at 5′ end of homologous arm for negative selection (Yanagawa et al., 1999). The linearized targeting vector was transfected into MS12 (C57BL/6J [B6]) ES cells. Positive clones were selected by Southern blots analysis, and then injected into Balb/c blastcysts. Offsprings harboring targeted allele were generated from the crossing of chimera mice with B6 mice and confirmed by Southern blots analysis. To generate a null allele, B6 eggs *in vitro* fertilized by F1 sperm were microinjected with circular plasmid DNA containing the Cre recombinase gene as described previously (Sunaga et al., 1997). After the confirmation of null allele by Southern blots analysis, heterozygous mice harboring null allele were intercrossed for obtaining the homozygous mice as Pael-R KO mice.

2.2. Generation of Pael-R Tg mice

Human platelet-derived growth factor β2 promoter-driven human Pael-R transgenic (PDGFβ-Tg) mice, and mouse prion protein promoter-driven Pael-R Tg (PrP-Tg) mice were generated using the human PDGF β2 vector (Chui et al., 1999) (kindly provided by Drs. Tanahashi H. and Tabira T., National Institute of Neuroscience, Japan), and MoPrP vector (Borchelt et al., 1996) (kindly provided by Drs. Borchelt D.R. and Fromholt D., Johns Hopkins University). The NotI fragments from the PDGFβ-Pael-R and the PrP-Pael-R plasmids were microinjected into B6 and C3H/B6 mouse eggs, respectively. Potential founders were identified using Southern blot analysis and PCR. Stable Tg lines were established by breeding founders to B6 mice (for PDGFβ-Tg) and C3H/B6 mice (for PrP-Tg).

2.3. Antibodies

Anti-Pael-R (#202) and anti-LP-2 (#23) monoclonal antibodies (mAbs) were raised in mice against the C-terminal 61 amino acids of human Pael-R and the C-terminal 62 amino acids of human ET_BR-LP2 (LP-2), respectively, expressed in bacteria. Anti-TH (MAB318) and anti-actin (MAB1501R) Abs were purchased from Chemicon. Anti-transferrin receptor (H68.4) and anti-NSE (BBS/NC/VI-H14) Abs were obtained from Zymed and Dako, respectively.

2.4. Western blots and immunohistochemistry

A crude homogenate was prepared by adding 10 μl of ice-cold buffer A (50 mM Tris–HCl, pH 7.5, 120 mM NaCl, 5 mM EDTA containing Complete Protease Inhibitors [Roche Diagnostics])/mg of brain tissue and using a Dounce homogenizer with a tight pestle (40 strokes). The suspension was fractionated by centrifugation at 1000 × *g* for 5 min and then by ultracentrifugation at 165,000 × *g* for 60 min. The pellet fraction was washed three times with buffer A, and then extracted by shaking in 5 μl of buffer B (buffer A containing 1% Triton X-100 and 1% SDS)/mg of brain tissue for 60 min at RT. After centrifugation at 18,500 × *g* for 30 min, the pooled supernatants were used as the total membrane fraction. Each fraction was Western blotted using ECL detection reagents (GE Healthcare). Protein was quantified using the Coomassie protein assay reagent (Pierce).

2.5. Animal treatment, drugs, and behavior

Three-month-old male littermates of heterozygous interbreedings were used in the 1-methyl-4-phenyl-1,2,3,6-tetrahydropyridine (MPTP) experiments. Mice received either two intraperitoneal injections of MPTP (Sigma; 10 h apart; 30 mg/kg each), or vehicle control (saline). The animal experiments described were approved by Animal Experiments Committee of RIKEN Brain Science Institute. All procedures were performed according to guidelines of RIKEN Brain Science Institute. Treatment with 6-hydroxydopamine (6-OHDA) was performed as described previously (Kaneko et al., 2000). In short, the male Tg or KO mice at 2–3 months of age and their littermates were deeply anesthetized with sodium pentobarbital (50 mg/kg i.p.). A needle was introduced into the left hemisphere using stereotaxic techniques, and phosphate-buffered saline (PBS, 0.5 μl) containing 6-OHDA hydrobromide (4 mg/ml) and 0.016% ascorbic acid was injected into two sites in the left striatum over 5 min. After 1 week (for the MPTP experiments) and 3 weeks (for the 6-OHDA experiments), mice were subjected to neurochemical analysis or counting of the number of tyrosine hydroxylase (TH)-positive neurons as follows. The brain perfused with cold PBS followed by 4% paraformaldehyde in PBS, was removed, embedded in paraffin, sectioned (12 μm), deparaffinized using standard protocols, and stained with anti-TH mAb (Chemicon, 1:100). The total number of TH-stained cells with clearly visible nuclear borders in the substantia nigra pars compacta was estimated in every fifth section, using a previously described unbiased stereological method (Nelson et al., 1996; West, 1999). A complete reduction of TH immunosignal in the striatum was also used to confirm that the injection sites of each animal were optimally located. For spontaneous locomotion activities, mice were placed in white chambers (50 cm × 50 cm). After introduction of mice without acclimation, horizontal migration up to 30 min was recorded by overhead CCD cameras and analyzed by Image OF4, a program based on the NIH image program (O'Hara & Co. Ltd., Tokyo, Japan).

2.6. Neurochemical analysis

Striatal tissue was homogenized in solution H (0.4 M $HClO_4$ containing 4 mM $Na_2S_2O_5$, 4 mM diethylenetriaminepentaacetic acid and 5 mM 1,4-dithiothreitol). The supernatant by centrifugation at 18,500 × *g* for 10 min was used for measurement of free catechols. The alumina extraction of free catechols was basically performed as described previously (Ito et al., 1988).

2.7. In vivo microdialysis

Mice were anesthetized with sodium pentobarbital and placed in a stereotaxic frame. Dialysis probes (membrane length, 2.0 mm; outer diameter,

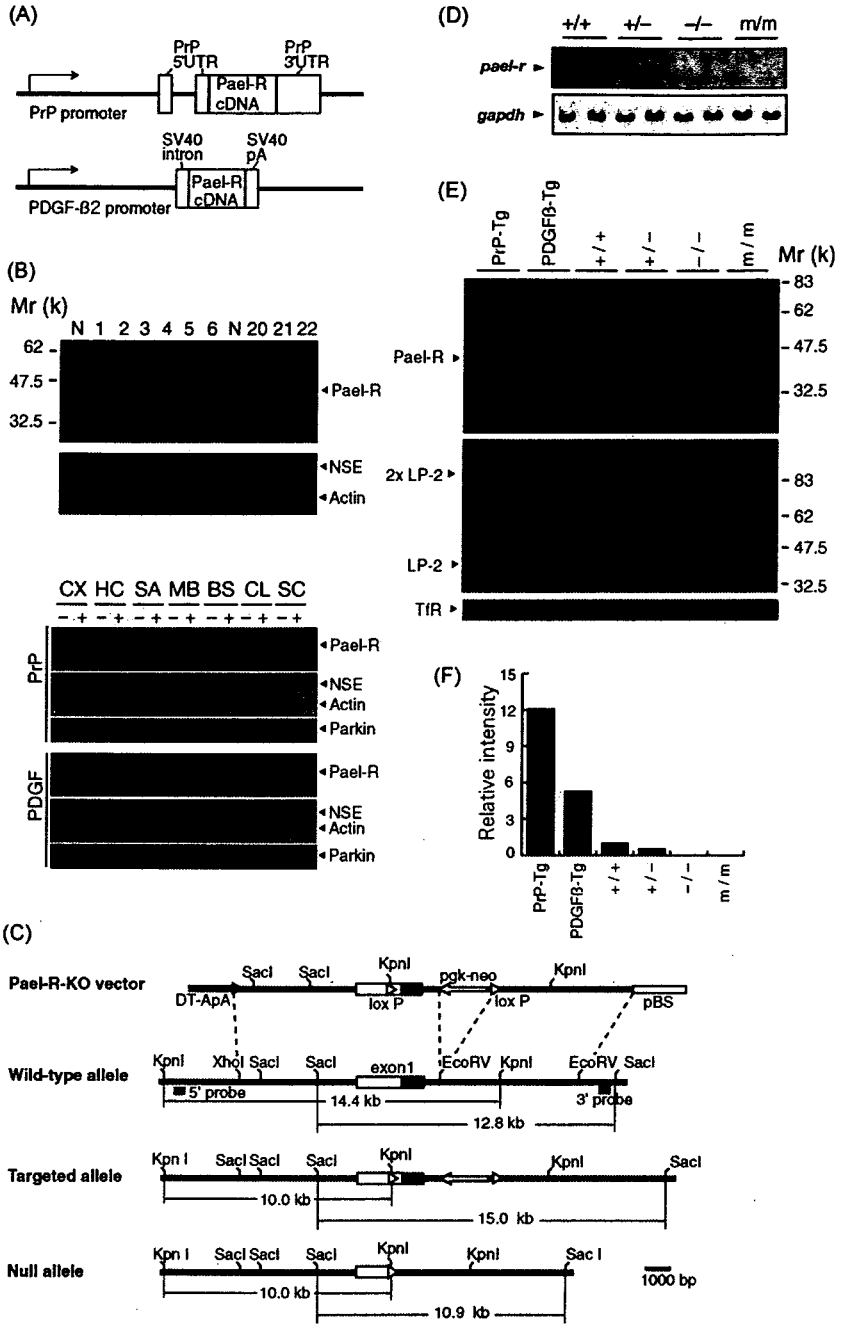

Fig. 1. Generation of Pael-R Tg and Pael-R KO mice. (A) Expression of the Pael-R gene was under the control of the PrP and PDGF β2 promoter. pA, polyadenylation sequence. (B) Expression levels of Pael-R in the whole brain of each PrP-Tg line (1–6), PDGFβ-Tg (20–22) and non-Tg mouse (N) are shown (upper). Expression levels of Pael-R and Parkin in each region of the brain of PrP-Tg line 1 and PDGFβ-Tg line 20 mice and their non-Tg littermates (lower). CX, cerebral cortex; HC, hippocampus; SA, striatum; MB, midbrain; BS, pons and medulla; CL, cerebellum, and SC, spinal cord. The amounts of neuron-specific enolase (NSE) and actin in each lane were shown as loading controls. (C) The murine Pael-R gene and targeting vector. A region of the Pael-R gene that includes the proximal exon 1 with a start codon is shown. Two loxP sites were inserted on the both sides of the Pael-R coding region within exon 1 (5′-UTR, white box; CDS1, gray box; a loxP site in the exon 1, 461 bp upstream from the translation initiation site). A *neo* cassette was inserted after exon 1. Locations of probes for southern blot analysis are indicated. DT-ApA, the diphtheria toxin gene with poly(A) sequence for negative selection; pBS, pBluescript (Stratagene). (D) Northern blot analysis of Pael-R transcripts (*pael-r*) in representative brain samples. '+', '−', and 'm' indicates the WT, null and targeted allele in (C), respectively. The same blot was hybridized with a *gapdh* probe as a loading control (*gapdh*). (E) Western blot analysis with the membrane fractions from the whole brain of 2.5-month-old mice. LP-2, ET_BR-LP2; 2× LP-2, a putative SDS-resistant dimer form of LP2; TfR, transferrin receptor. (F) Quantitative analysis of expression levels of Pael-R protein normalized against each TfR level in (E). The mean amounts of Pael-R in WT (+/+) are defined as one.

0.22 mm; D-I-6-02, Eicom, Kyoto, Japan) were implanted in the left striatum. The stereotaxic coordinates for implantation of microdialysis probes were anterior–posterior, 0.26 mm; dorsal–ventral, 3.5 mm; and lateral, 2.0 mm relative to the bregma (Goldberg et al., 2003). Placement of the probe was verified by histological examination subsequent to the experiments. Following surgery, animals were returned to their home cages and given free access to food and water. Twenty hours later, to avoid transient changes, if any, caused by surgical damage, the dialysis probe was connected to a syringe pump and

perfusion was carried out at 1.0 μl/min with artificial striatal cerebrospinal fluid (aCSF: Na^+, 155.0 mM; Ca^{2+}, 1.1 mM; K^+, 2.9 mM; Mg^{2+}, 0.8 mM; and Cl^-, 155.6 mM; pH 7.4). After a 4-h equilibration period, the perfusates were collected every 30 min. The basal level of DA was determined by averaging the DA levels of eight dialysates collected during a 4-h period. The DA level due to Ca^{2+}-dependent efflux was the difference between the basal level and the average level in two consecutive dialysates collected within 1 h after perfusion of Ca^{2+}-free aCSF for 2 h. Samples were assayed for DA or DOPAC using HPLC-EC.

2.8. Electrophysiology

The midbrain slices and corticostriatal slices prepared from 3–4-week-old mice were cut coronally and parasagittally, respectively (250 μm thick), transferred to an incubation chamber and allowed to recover for 1 h before recording. During recording, a slice was perfused continuously with aCSF (124 mM NaCl, 3 mM KCl, 1 mM NaH_2PO_4, 1.2 mM $MgCl_2$, 2.4 mM $CaCl_2$, 10 mM glucose, 26 mM $NaHCO_3$, pH 7.4) saturated with 95% O_2, and 5% CO_2 at a rate of 1–2 ml/min at 30 °C. Whole-cell patch-clamp recordings were made from DA neurons in midbrain slices or striatal medium spiny neurons (MSNs) in corticostriatal slices by an EPC9/2 amplifier (HEKA Elektronik Lambrecht/Pfalz, Germany) with infrared differential contrast visualization using an Olympus BX50WI (Tokyo, Japan) and a CCD camera. For current-clamp recordings, patch pipettes contained 129 mM K-gluconate, 11 mM KCl, 2 mM $MgCl_2$, 10 mM HEPES, 4 mM Na_2-ATP, 0.3 mM GTP, and 0.5% biocytin (brought to pH 7.3 with KOH; osmolarity 280 mOsm). Hyperpolarizing and depolarizing current injection was made to study the physiological properties of DA neurons. For voltage-clamp recordings, patch pipettes (4–6 MΩ) were filled with 124 mM Cs-methanesulfonate, 11 mM KCl, 2 mM $MgCl_2$, 10 mM HEPES, 4 mM Na_2-ATP, 0.3 mM GTP, 0.1 mM spermine, 5 mM QX-314, and 0.5% biocytin and brought to 280 mOsm and pH 7.3 with CsOH. Inhibitory postsynaptic currents (IPSCs) were evoked by electrical stimulation of the striatum with a bipolar tungsten electrode in the presence of the *N*-methyl-D-aspartate receptor antagonist *D*(−)-2-amino-5-phosphonopentanoic acid (D-AP5, 25 μM) and the α-amino-3-hydroxy-5-methyl-4-isoxazolepropionic acid receptor antagonist 6-cyano-7-nitroquinoxaline-2,3-dione (CNQX, 20 μM). Effects of paired pulse stimulation were then investigated by delivering five pairs of stimuli at decreasing intervals (500, 200, 100, 50, and 25 ms). Thirty stimulus pulses given 70 ms apart (about 14 Hz) were next applied three times every 20 s. Nomifensine (3 μM), an uptake inhibitor of DA, was then bath-applied. Voltage errors attributable to the liquid junction potential (11 mV) were subtracted. Signals were filtered at 5 kHz and digitized at 20 kHz with Pulse/PulseFit (HEKA). If series resistance was changed by >20%, the experiments were discarded. To confirm the morphology of the recorded neurons, the slices containing biocytin-filled cells were fixed and stained with Vectastain ABC kit (Vector Laboratories). Areas of cell bodies of DA neurons were measured using NIH Image J software (http://rsb.info.nih.gov/ij/). Statistical significance was assessed by unpaired or paired Student's *t*-tests. D-AP5 was obtained from Tocris Cookson and all other drugs from Sigma.

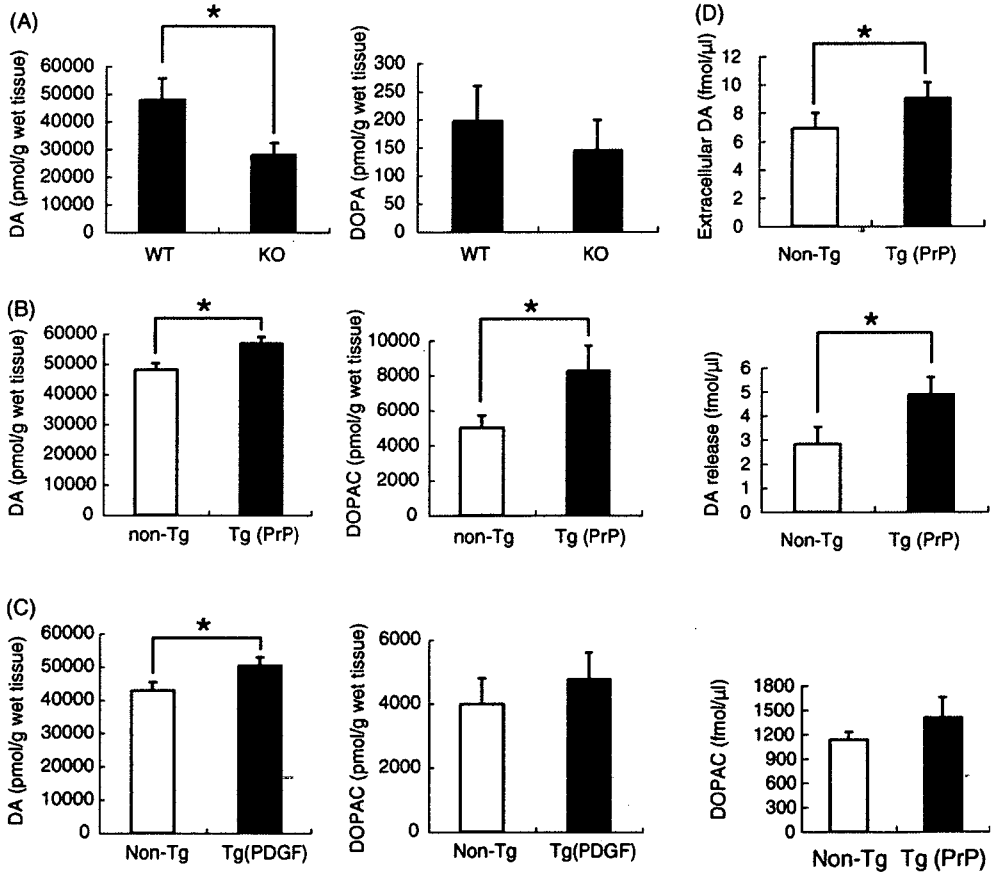

Fig. 2. DA and its metabolites in the striatum of Pael-R Tg and Pael-R KO mice. (A) Striatal tissue levels of DA (left) and L-DOPA (right) in Pael-R KO and WT littermate mice measured by HPLC-EC ($n = 6$ each). Results are presented as the mean ± S.E.M. for six animals at 13-months of age. $^*P < 0.05$ *vs.* WT by Student's *t*-test. (B) Striatal tissue levels of DA and DOPAC in PrP-Tg and non-Tg littermate mice measured by HPLC-EC. Results are presented as the mean ± S.E.M. for 15 animals at 10-months of age. $^*P < 0.05$ *vs.* non-Tg by Student's *t*-test. (C) Striatal tissue levels of DA and DOPAC in PDGFβ-Tg and non-Tg littermate mice measured by HPLC-EC. Results are presented as the mean ± S.E.M. for 12 animals at 15 months of age. $^*P < 0.05$ *vs.* non-Tg by Student's *t*-test. (D) Extracellular DA levels (upper), DOPAC levels (lower), and Ca^{2+}-dependent DA release (middle) in the striatum of free moving PrP-Tg and non-Tg littermate mice at 10 months of age measured by microdialysis (mean ± S.E.M., $n = 10$ each). $^*P < 0.05$ *vs.* non-Tg by Student's *t*-test.

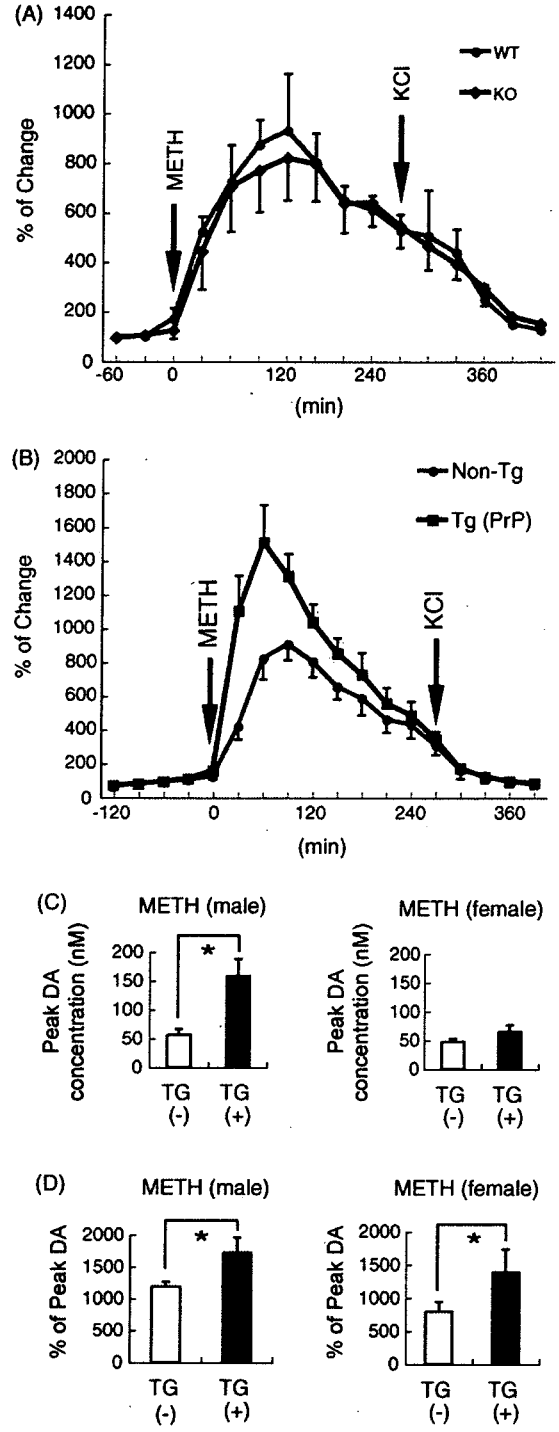

Fig. 3. Hypersensitivity to methamphetamine in Pael-R Tg mice. (A) Time course of DA release in the striatum of Pael-R KO ($n = 8$) and WT littermate mice ($n = 8$) in response to methamphetamine (METH, 30 mg/kg, s.c.). Perfusion of medium containing 100 mM KCl through the microdialysis probe at 270 min after METH stimulation did not show another peak of DA release, suggesting that almost all of the intracellular DA was released by this METH administration. The values are represented as the mean ± S.E.M. of percentage to basal levels (average of the levels at 30 and 60 min before METH administration) for eight animals at 6–12 months of age. (B) Time course of DA release in the striatum of PrP-Tg ($n = 10$) and non-Tg littermate mice ($n = 10$) in response to METH (30 mg/kg, s.c.) and subsequent KCl (100 mM) administration as in (A). The values for 10 animals at 6 months of age are represented as in (A). DA release after METH stimulation in PrP-Tg was significantly different by repeated measures ANOVA [genotype × time interaction, $F(1,245) = 27.1$; $P < 0.001$]. (C) The peak values of striatal DA efflux after METH treatment in PrP-Tg male (left, $n = 5$ each group) and female (right, $n = 5$ each group) mice are shown. *$P < 0.05$ *vs.* non-Tg by Student's *t*-test. (D) Percent of the peak DA efflux to basal DA content after METH treatment in PrP-Tg male (left, $n = 5$ each group) and female (right, $n = 5$ each group) mice is shown. *$P < 0.05$ *vs.* non-Tg by Student's *t*-test.

3. Results

3.1. Generation of Pael-R Tg and Pael-R KO mice

Tg mice were generated expressing human Pael-R under the control of the PrP promoter and the PDGF β2 promoter (Fig. 1A). Several lines of Tg mice were obtained, and mice with the highest expression levels of Pael-R were chosen from each promoter group and characterized (Fig. 1B). The PrP promoter-driven transgenic (PrP-Tg) line PrP1 (maintained on a mixed genetic background of C3H × B6), showed high expression of Pael-R transgene in the whole brain, while the PDGF β2 promoter-driven transgenic (PDGFβ-Tg) line 20 on a B6 background showed marked expression in the striatum and the midbrain compared with other regions (Fig. 1B). The expression of Pael-R transgene in TH-positive neurons in the SN was immunohistochemically confirmed by increased Pael-R immunosignals compared with that of non-Tg mice (data not shown).

Murine Pael-R gene contains two exons (Marazziti et al., 1998). The first exon containing a start codon was targeted to generate Pael-R-deficient mice on a B6 background. Two loxP sites flanking exon 1 and a selection marker cassette were introduced into the mouse Pael-R gene by means of homologous recombination in ES cells (Fig. 1C, targeted allele). To generate a null allele, part of the exon 1 and the selection marker were removed by *in vitro* fertilization using sperm from a heterozygote mouse bearing the targeted allele and subsequent microinjection of Cre recombinase cDNA into the fertilized eggs. Homologous recombination of the targeting construct and the deletion of the floxed cassette were confirmed by Southern blotting (data not shown). To determine the level of expression of Pael-R transcripts, Northern blotting analysis was performed with total RNA from whole brain samples (Fig. 1D). This analysis indicated that in mice carrying both the targeted and null alleles, the expression of Pael-R mRNA transcripts is completely lost, suggesting that the insertion of loxP or the selection cassette on non-coding regions has disrupted a critical element(s) for transcripton.

The protein levels of expression in Pael-R Tg and KO mice were assessed by Western blotting with membrane fractions prepared from whole brain of samples with anti-Pael-R Ab (Fig. 1E). PrP-Tg and PDGFβ-Tg mice had respectively ~12 and ~5.5 times higher Pael-R protein levels compared with normal mice (+/+), while homozygote mice bearing the null allele or targeted allele failed to show an immunosignal of the Pael-R protein (Fig. 1E and F) The alterations of Pael-R expression had no effect on the expression of LP-2, whose gene has the highest homology with the Pael-R gene (Fig. 1E) (Valdenaire et al., 1998).

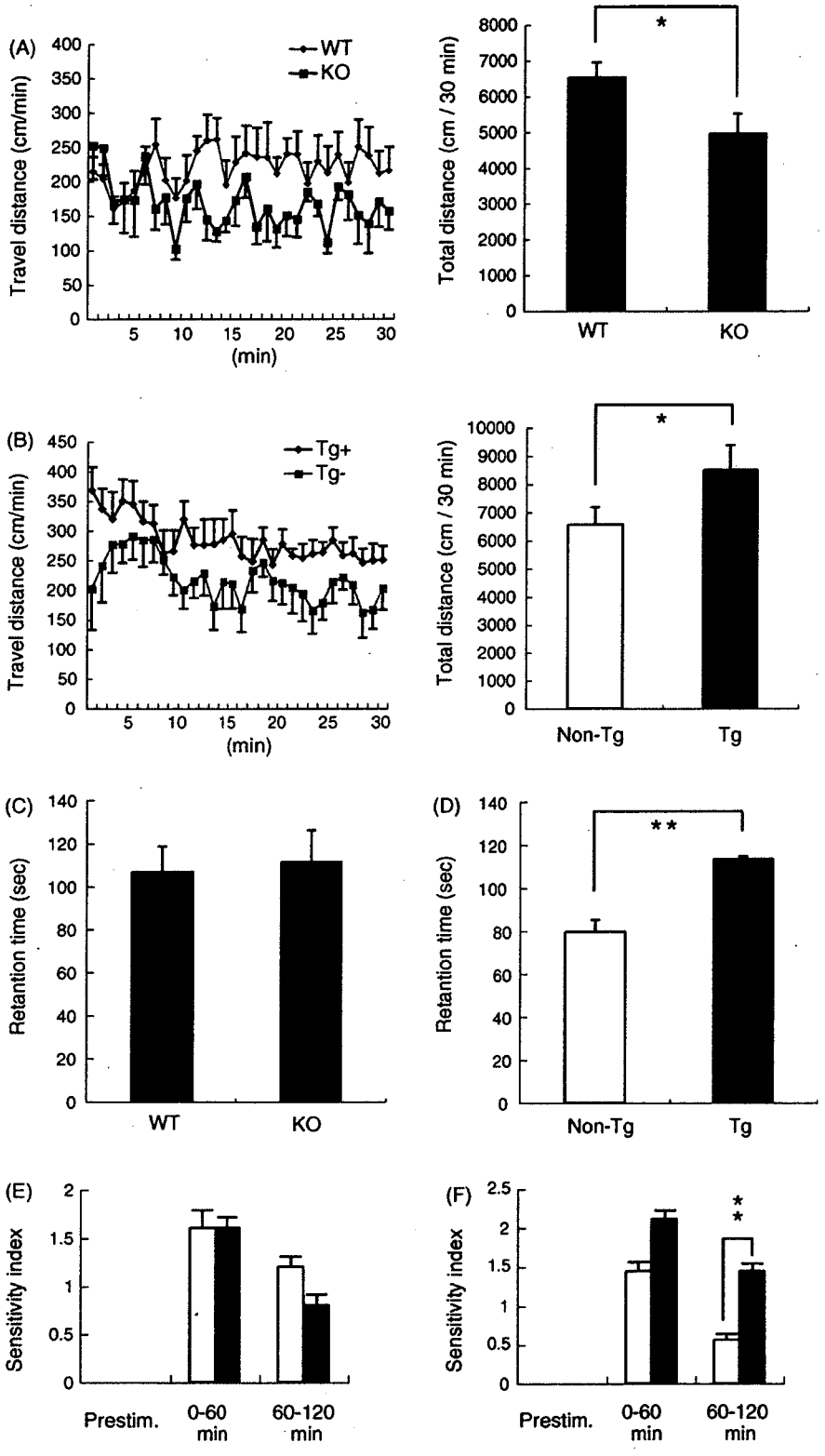

Fig. 4. Locomotor activity of Pael-R Tg and Pael-R KO mice. (A) Spontaneous horizontal migration of Pael-R KO ($n = 9$) and WT littermate ($n = 11$) mice at 1 year of age over a period of 30 min just after introduction into the open field chamber (50 cm × 50 cm). The migration distance in each minute interval after introduction (left) and total migration distance (right) are represented as mean ± S.E.M. (*$P < 0.05$ *vs.* WT; Student's *t*-test). (B) Spontaneous horizontal migration of PrP-Tg ($n = 11$) and non-Tg littermate ($n = 9$) mice at 1 year of age over a period of 30 min as in A. *$P < 0.05$ *vs.* non-Tg by Student's *t*-test. (C) Motor coordination of Pael-R KO and WT littermate mice at 1 year of age was assessed with the rotarod test ($n = 10$ each group). The retention time on a rotating wheel was consecutively measured four times. Each trial lasted for a maximum of 5 min, during which time the wheel rotates with a linear acceleration from 4 to 40 rpm. Data are represented as mean ± S.E.M. of retention time. (D) Motor coordination of PrP-Tg and non-Tg mice at 1 year of age was assessed with the rotarod test as in (C). (**$P < 0.01$ *vs.* non-Tg; Student's *t*-test, $n = 10$ each group). (E) The behavior of Pael-R KO and WT littermate male mice ($n = 5$ each group) during the free moving *in vivo* microdialysis analysis before and after METH administration (30 mg/kg) in Fig. 3A was scored as follows: 0, none; 1, piloerection without rotational motion; 2, slow rotational motion; 3, fast rotational motion or jumping movement. Mean ± S.E.M. of the score are represented as Sensitivity Index. Grey bars, KO mice; white bars, WT

3.2. Abnormal DA synthesis and metabolism by altered Pael-R expression

Pael-R Tg and KO mice are viable and present no gross anatomical abnormalities. Pael-R KO mice gained weight normally, whereas Pael-R Tg mice gained at a slower rate (37.1 ± 4.1 g in PrP-Tg *versus* 47.1 ± 2.1 g in PrP-non-Tg males at 10 months, $P < 0.05$, $n = 7$; 30.6 ± 1.9 g in PrP-Tg *versus* 38.5 ± 2.4 g in PrP-non-Tg females at 10 months, $P < 0.01$, $n = 14$; and 23.0 ± 1.7 g in PDGFβ-Tg *versus* 30.2 ± 1.8 g in PDGFβ-non-Tg males at 6 months, $P < 0.05$, $n = 9$).

Because Pael-R is abundantly expressed in the DA neurons and is implicated in the pathogenesis of PD, we then examined the effect of altered Pael-R expression on the nigrostriatal pathway. In the whole striatum tissue of Pael-R KO mice, DA, but not its precursor L-DOPA, levels were reduced to 60% of that in wild-type (WT) littermates (Fig. 2A). In contrast, striatal levels of DA were increased in both strains of Pael-R Tg mice (Fig. 2B and C). The levels of DOPAC were significantly increased only in PrP-Tg mice (Fig. 2B and C). In PrP-Tg mice, the concentration of extracellular DA (measured by *in vivo* microdialysis of freely moving mice) in the striatum as well as the concentration due to Ca^{2+}-dependent release at the presynapse of DA neurons was increased (Fig. 2D). The concentrations of extracellular DA and DOPAC (measured by *in vitro* microdialysis) were not significantly different in the striatum of Pael-R KO mice (data not shown).

3.3. Increased DA storage and release in Pael-R Tg mice

Administration of the psychostimulant methamphetamine (METH) stimulates DA release from the presynapse of DA neurons. METH administration (30 mg/kg, s.c.) induced a similar increase in extracellular DA levels in Pael-R KO and WT littermate mice (Fig. 3A). No increase occurred when 100 mM KCl was infused intrastriatally *via* a microdialysis probe at 270 min after METH, suggesting that 30 mg/kg METH is sufficient to the release of almost all DA stored in the presynapse. By contrast, METH administration (30 mg/kg, s.c.) stimulates a significant increase (~1.6-fold) in extracellular DA level in PrP-Tg compared with non-Tg mice ($P < 0.001$ by repeated measures ANOVA; Fig. 3B). Following METH administration, dialysate levels of DOPAC were decreased similarly in both PrP-Tg and PrP-non-Tg mice as well as Pael-R KO mice (data not shown), suggesting that METH inhibits monoamine oxidase activity as previously reported (Fumagalli et al., 1998). Although actual value of DA efflux was larger in male mice than in female mice, there was no sex difference in the ratio of peak DA levels to basal DA levels (Fig. 3C and D).

3.4. Behavioral phenotype by mice with altered Pael-R expression

DA content in the striatum plays an important role in the control of locomotor and stereotypic behavior. Changes in DA levels in these mice led us to test locomotor activity. The spontaneous locomotor activity of naïve Pael-R KO mice was significantly reduced in an initial 30-min trial (Fig. 4A). However, whereas the locomotor activity of Pael-R KO mice did not change every month, that of WT littermates gradually declined, probably because of habituation to the test. Consequently, locomotor activity was higher in Pael-R KO mice than WT littermates 5 months later (data not shown). The result suggests that Pael-R KO mice somewhat lose the ability of habituation to a circumstance. In contrast to Pael-R KO mice, both PrP-Tg and PDGFβ-Tg mice showed elevated locomotor activity in the same test (Fig. 4B and data not shown).

Motor performance was assessed by the rotarod test as described previously (Tateno et al., 2004). The rotarod scores measured of 6-month-old and 1-year-old Pael-R KO mice were not significantly changed whereas 1-year-old PrP-Tg showed the significant improvement in this test (Fig. 4C and D and data not shown). The phenotypes of Pael-R Tg mice in the locomotor test and the rotarod test might be suggested to reflect an elevated extracellular DA content.

Behavior in response to the METH-treatment (30 mg/kg, s.c.) was assessed in Pael-R KO mice and PrP-Tg mice (Fig. 4E and F). The responses to METH of Pael-R KO male mice did not significantly differ from that of their WT male littermates (Fig. 4E). However, these responses were more sensitive in PrP-Tg mice than in non-Tg littermates (Fig. 4F). These results correlated well with the DA release data obtained in the *in vivo* microdialysis experiment (Fig. 3A and B). The female responses tended to be milder than male, although levels of Pael-R protein expression in the brain were not different between male and female PrP-Tg mice (data not shown).

3.5. Sensitivity to DA neurotoxins

The numbers of TH-immunoreactive neurons in the SN, the ventral tegmental area (VTA) and the locus coeruleus of Pael-R KO and PrP-Tg mice (which are highly expressed in the locus coeruleus as well as the SN and VTA unlike PDGFβ-Tg mice) showed age-dependent loss of TH-positive neurons (manuscript in submission). The number of TH neurons in Pael-R KO mice showed a slight reduction compared with their WT littermates (Fig. 5A). However, the number did not change over time, suggesting that Pael-R somewhat contribute to developmental regulation of TH-positive neurons (data not shown).

Parkin KO mice have an increased extracellular DA and whole striatal DOPAC levels (Goldberg et al., 2003; Itier et al., 2003). Both Parkin KO mice and Pael-R Tg mice appear to have

littermates; Prestim., before METH-treatment; 0–60 min, for the first 1 h of METH-treatment; 60–120 min, for the second 1 h. (F) The behavior of PrP-Tg and non-Tg mice ($n = 5$ males; $n = 4$ females in each genotype) in METH administration (30 mg/kg) was scored as in (D). The score representing the sensitivity to METH is higher in the second 1 h after METH administration compared with non-Tg littermate (**$P < 0.01$ by Mann–Whitney U-test). Black bars, Tg mice; and white bars, non-Tg littermates.

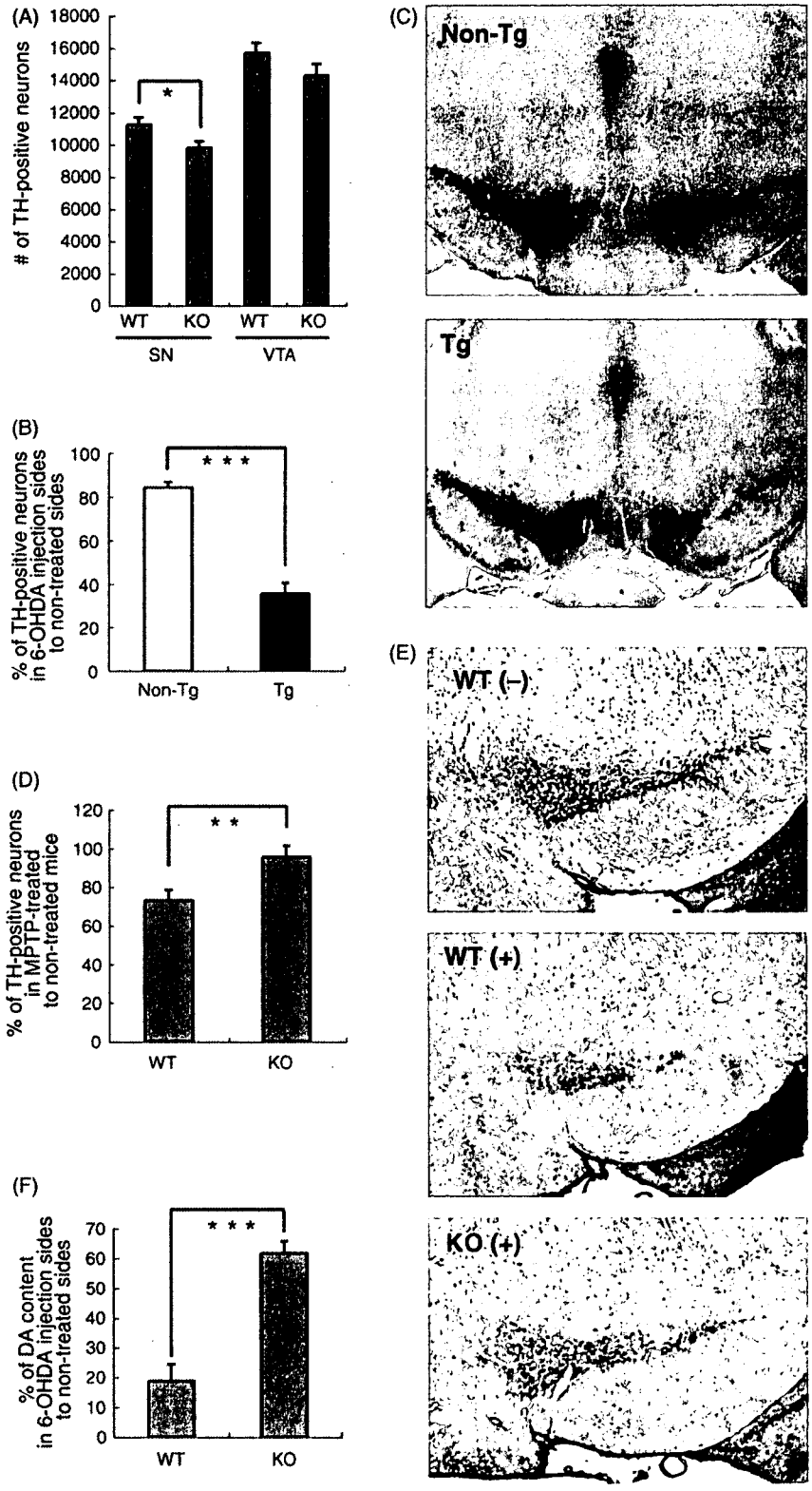

Fig. 5. Sensitivity of DA neurons to the neurotoxins in Pael-R Tg and Pael-R KO mice. (A) The estimated number of TH-positive neurons in the SN and VTA of Pael-R KO and WT littermate mice at 3 months of age was assessed by a stereological method (mean ± S.E.M., $n = 7$ mice). *$P < 0.05$ *vs.* WT littermates by Student's *t*-test. (B) Effect of 6-OHDA on DA neurons of Pael-R Tg mice 21 days after administration. 6-OHDA was injected into the left striatum of PrP-Tg and non-Tg littermate mice at 2–3 months of age. The number of TH-immunopositive neurons in the SN was assessed by a stereological method. To correct for genotype-based differences in the number of TH-positive cells, data are represented as percentage of the number on the non-treated side (right striatum) of each animal (mean ± S.E.M., Tg, $n = 8$; non-Tg, $n = 9$). ***$P < 0.001$ *vs.* non-Tg by Student's *t*-test. (C) Representative coronal sections of 6-OHDA-treated non-Tg (upper) and Tg (lower) brains containing the SN are shown. The 6-OHDA-treated SN is located on the left side. (D) Effect of MPTP on DA neurons of Pael-R KO mice 7 days after administration. MPTP was injected into Pael-R KO and WT littermate mice at 3 months of age. Data are represented as percentage of the number of DA neurons in the SN in each pair with saline treatment (mean ± S.E.M., $n = 8$ per each group). **$P < 0.01$ *vs.* non-Tg by Student's *t*-test. (E) Representative coronal sections of

this phenotype. Although DA neurons in the SN of Parkin KO mice do not show axonal degeneration or neuronal death with age like those of AR-JP patients, there is some evidence that DA neurons in Parkin KO mice are functionally disturbed. Therefore, we expected that DA neurons in Pael-R Tg mice might be subjected to stress to deal with elevated DA content. DA neurotoxins 6-OHDA and MPTP, which have been used to develop PD animal models, behave as catecholaminergic or DA neuron-specific neurotoxins (Betarbet et al., 2002). To evaluate the vulnerability of mice with altered Pael-R expression to these neurotoxins, the number of TH-immunopositive neurons in the SN or the amounts of DA in the striatum was evaluated after the treatment. The SN of PrP-Tg and non-Tg littermates that were treated with 6-OHDA-injection into the left striatum showed, respectively, 64% and 16% reduction of TH-immunopositive neurons compared with the untreated hemisphere (Fig. 5B and C). In contrast, MPTP-treatments of WT and Pael-R KO mice led to 27% and 4% fewer TH-immunoreactive neurons, respectively, than counted in saline-treated WT mice (Fig. 5D and E). The amount of striatal DA in Pael-R KO mice and WT littermates 3 weeks after 6-OHDA-injection into the left striatum showed, respectively, 38% and 81% reduction compared with the untreated hemisphere (Fig. 5F). These results indicate that DA neurons in PrP-Tg mice are more sensitive to DA neurotoxins, suggesting that these DA neurons are potentially stressed. Conversely, DA neurons in Pael-R KO mice appeared to be less sensitive (i.e., to have the opposite characteristics from that in PrP-Tg mice).

3.6. Electrophysiological analysis of DA neurons in Pael-R-KO and PrP-Tg mice

To study how the function of DA neurons was influenced by the expression of Pael-R, we made the whole-cell patch-clamp recordings from DA neurons in midbrain slices and slices containing the striatum prepared from Pael-R KO and PrP-Tg mice of postnatal 3–4 weeks. In both DA neurons of Pael-R KO (WT, $n = 36$ cells, KO, $n = 39$ cells) and PrP-Tg (non-Tg, $n = 28$ cells, Tg, $n = 28$ cells) mice we found no changes in the resting membrane potentials (WT, -55.4 ± 0.8 mV, KO, -55.0 ± 0.7 mV; non-Tg, -57.2 ± 0.9 mV, Tg, -55.3 ± 1.2 mV), the spike thresholds (WT, -30.0 ± 0.5 mV, KO, -29.8 ± 0.6 mV; non-Tg, -29.5 ± 0.5 mV, Tg, -30.4 ± 0.4 mV), the peak values (WT, 26.9 ± 1.1 mV, KO, 26.8 ± 1.1 mV; non-Tg, 27.8 ± 1.3 mV, Tg, 27.3 ± 1.3 mV), and amplitudes (WT, 56.9 ± 1.0 mV, KO, 56.6 ± 1.3 mV; non-Tg, 57.4 ± 1.2 mV, Tg, 57.6 ± 1.3 mV) of action potentials, the spike widths at half amplitude (WT, 1.46 ± 0.05 ms, KO, 1.47 ± 0.06 ms; non-Tg, 1.57 ± 0.06 ms, Tg, 1.53 ± 0.06 ms), spontaneous firing frequencies (WT, 2.87 ± 0.20 Hz, KO, 2.50 ± 0.20 Hz; non-Tg, 1.85 ± 0.13 Hz, Tg, 1.81 ± 0.15 Hz), and firing patterns. However, the input resistance of DA neurons of PrP-Tg mice was slightly larger (Student's t-test, $P < 0.05$; Fig. 6A) than that of the non-Tg control neurons although there was no difference between DA neurons of Pael-R KO and WT mice (data not shown). Interestingly, the input resistance in the striatal MSNs was smaller in Pael-R KO mice (WT, $n = 16$, 133.3 ± 18.9 MΩ; KO, $n = 14$, 57.6 ± 9.8 MΩ, $P < 0.01$) and larger in PrP-Tg mice (non-Tg, $n = 19$, 81.9 ± 22.3 MΩ; Tg, $n = 22$, 146.2 ± 21.4 MΩ, $P < 0.05$) than their respective controls (data not shown). Since the factors which determine the input resistance are the cell size and the density and permeability of various types of ion channels incorporated into the cell membrane, our finding that the cell size of the Tg DA neurons was similar to that of non-Tg controls (soma area: non-Tg, 303 ± 14 μm^2, $n = 29$; Tg, 286 ± 16 μm^2, $n = 26$; $P > 0.4338$) suggests a possible interaction of Pael-R with a certain membranous component.

Electrical stimulation of cortico- and nigro-striatal pathways in striatal slices evokes release of DA from the residual dopaminergic nerve terminals (Calabresi et al., 1995). The released DA then depresses GABAergic IPSC in the striatal MSNs by activation of presynaptic DA D2 receptors (Bamford et al., 2004; Centonze et al., 2002, 2003, 2004). We thus performed paired pulse stimulation to get paired pulse ratios (PPRs) of the second IPSC amplitudes to the first in the MSN to study a change in DA release in Pael-R KO and PrP-Tg mice. We found no statistical change in PPRs in both Pael-R KO and PrP-Tg mice with respect to their respective controls (upper left in Fig. 6B, and data not shown). Nomifensine is a selective DA uptake inhibitor interacting with the DA transporter at a site different from that of cocaine. A previous report demonstrated that both cocaine and amphetamine, more potent drugs than nomifensine, increased the DA content and suppressed IPSCs through activation of presynaptic DA D2 receptors (Centonze et al., 2002; Wieczorek and Kruk, 1994). After nomifensine application there was a slight increase in PPR in WT and a decrease in KO at an interval of 100 ms, yielding a significant difference only in Pael-R KO mice (lower left in Fig. 6B, $P < 0.05$). Furthermore, we found a significant decrease in IPSC amplitudes upon repeated low frequency stimulation (30 pulses applied 70 ms apart) both before and after application of nomifensine in Pael-R KO mice (right in Fig. 6B). In contrast, no change was observed in PPRs and IPSC amplitudes with paired pulse stimulation and repeated low frequency stimulation before and after nomifensine in PrP-Tg mice (data not shown). In both types of mice there were no changes in rise time and decay time constant of IPSC, suggesting no alterations in $GABA_A$ receptor channel kinetics *per se* (data not shown).

These results suggest that in Pael-R KO mice DA is significantly less released while electrophysiological properties of DA neurons remain unchanged. On the other hand, we did not observe any significant changes in DA neurons of PrP-Tg mice except for a small increase in input resistance probably because

MPTP-treated (+) or saline-treated (−) brains containing the SN are shown. (F) Effect of 6-OHDA on DA neurons of Pael-R KO mice. 6-OHDA was injected as in B at 2–3 months of age. The amount of DA in the striatum was measured by HPLC-EC method 21 days after administration. To correct for genotype-based differences in the amount of striatal DA, data are represented as percentage of the amount on the non-treated side (right striatum) of each animal (mean ± S.E.M., Tg, $n = 5$; non-Tg, $n = 5$). ***$P < 0.001$ *vs.* non-Tg by Student's t-test.

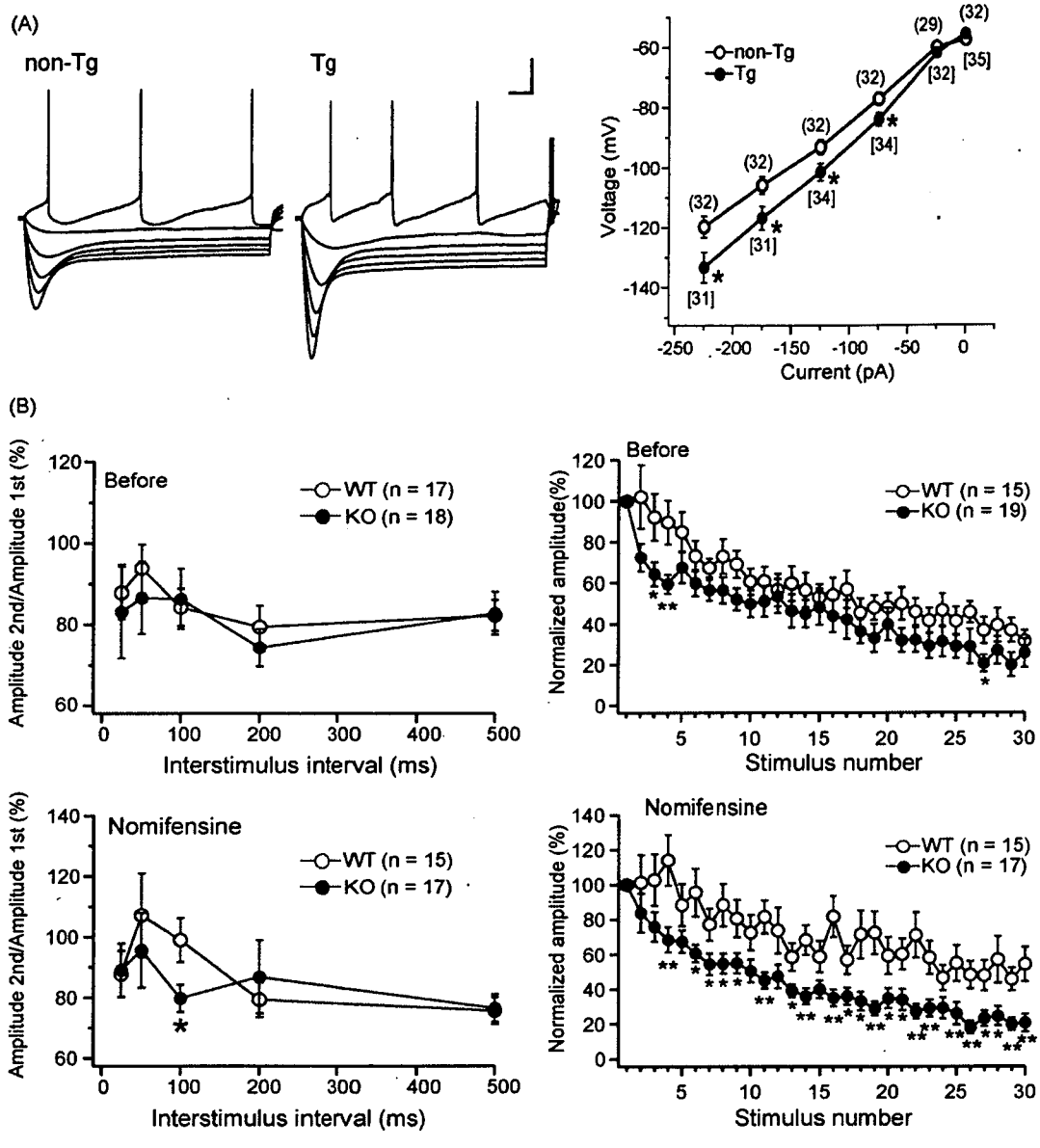

Fig. 6. Effects of Pael-R expression on physiological properties of DA neurons. (A) Sample waveforms of DA neurons taken from a non-Tg and a PrP-Tg mouse (left). Current–voltage relationships generated by injecting current pulses and recording the voltage deflections are shown on the right. Numbers in parenthesis show the numbers of cells sampled. Calibration, 25 mV, 100 ms. Input resistance in PrP-Tg mice is larger than that in non-Tg mice. *$P < 0.05$. (B) Effects of paired pulse stimulation and repeated low frequency stimulation before and after nomifensine in Pael-R KO mice. At left are shown plots of the mean (±S.E.M.) percentage of the second IPSC with respect to the first IPSC as a function of interstimulus interval before (upper) and after (lower) nomifensine application. After nomifensine treatment (3 μM), paired pulse depression (PPD) observed in wild types (WT, open circles) changed into small paired pulse facilitation (PPF), whereas PPD in knockouts (KO, gray circles) remained unchanged, yielding significant difference in paired pulse ratios at 100 ms ($P < 0.05$). Amplitudes (mean ± S.E.M.) of successive IPSCs in a burst of 30 applied 70 ms apart (i.e. at 14 Hz) normalized with respect to the amplitude of the first IPSC of the burst are shown on the right. There was a significant decrease in normalized IPSC amplitude in Pael-R KO mice (Student's *t*-test, $P < 0.05$) both before (upper) and after (lower) nomifensine treatment.

the change in DA content at this stage may be too small to detect nigrostriatal abnormalities in our electrophysiological analysis.

4. Discussion

Pael-R, transcripts of which are exclusively expressed in the CNS and testis, is a putative G protein coupled receptor (Donohue et al., 1998; Kawasawa et al., 2003). Unfolded Pael-R is thought to have a role in the etiology of AR-JP (Imai et al., 2001; Yang et al., 2003). Moreover, Pael-R-immunoreactivity has been observed in Lewy bodies of PD patients (Murakami et al., 2004). These reports suggest that unfolded Pael-R is associated with degeneration of DA neurons in PD. However, the physiological function of Pael-R in the CNS remains unknown. Our investigation of Pael-R-deficient and Pael-R Tg mice here revealed its physiological function as well as its pathological function in nigrostriatal system.

Although in Pael-R-deficient mice the number of TH-positive neurons in the SN was only slightly reduced, the striatal level of DA was significantly reduced. The alteration of DA content in these mice cannot simply be explained by a change of TH (a rate-limiting enzyme of DA synthesis, converting tyrosine into

L-DOPA) or aromatic amino acid decarboxylase (AADC, the enzyme that converts L-DOPA to dopamine) expression at protein level because the change of those expressions was not observed by Western blot analysis (data not shown). We also failed to detect a significant difference in the steady state and METH-stimulated levels of DA in the striatal CSF of Pael-R KO mice or a behavioral difference following METH administration. Thus, the reduction in whole striatal DA content could come from a non-releasable pool of DA in DA neurons.

The observations of Pael-R KO mice by Marazziti et al. (2004) is almost consistent with the results of our Pael-R KO mice. However, we do not see a significant reduction in the body weights of Pael-R KO mice and a significant defect of motor performance in the rotarod test. Another difference is their mice were supersensitive to amphetamine as assessed by locomotor activity, whereas we failed to find a significant difference in the amount of METH-stimulated DA in the CSF of Pael-R KO mice. These inconsistencies may come from tested ages of the mice and a difference in genetic backgrounds (100% C57BL/6J in this study *versus* 75% C57BL/6J and 25% 129P2/OlaHsd mixed background in the previous study by Marazziti's group). We analyzed older mice (12-month-old for measurement of body weight and rotarod test, 6–12-month-old for METH administration) compared with those (2.5–4-month-old) in Marazziti's group. As a result, a compensation for Pael-R-deficiency may go on with age.

The electrophysiological analysis was done only in young mice (3–4-week-old) for technical reasons. We found that the DA neuron and striatal MSN input resistance significantly increased in PrP-Tg mice and striatal MSN input resistance significantly decreased in Pael-R KO although the resting membrane potentials, the firing thresholds, and the amplitudes and widths of the spikes remained unchanged. This observation suggests that Pael-R may interact with certain membrane factor(s) that determine the input resistance and thereby play an important role in membrane constitution. On the other hand, the finding that PPR was not altered in either Pael-R Tg or KO mice indicates that Pael-R does not affect the GABA release machinery. However, the decrement of PPR was evident after nomifensine treatment and after repeated low frequency stimulation in Pael-R KO mice compared with WT littermates. This result indicates that the absence of Pael-R depletes available striatal DA content, which might be consistent with a very recent report that the population of the cell-surface DAT at the presynapse of Pael-R KO mice is increased by the absence of direct interaction between Pael-R and DAT (Marazziti et al., 2007). Another recent study on a candidate of Pael-R ligands has showed that Pael-R is internalized upon stimulation by a neuropeptide head activator (HA) (Rezgaoui et al., 2006). Given that Pael-R is one of DAT-associated proteins, the cell-surface DAT may be internalized together with Pael-R upon HA stimulation. That could cause the extracellular accumulation of DA. However, the observations that Pael-R KO mice and Pael-R Tg mice are respectively resistant and susceptible to DA neurotoxins suggest that there are DAT-independent mechanisms of MPTP toxicity.

Growing numbers of reports have shown that increased DA levels affect terminal degeneration of DA neurons and that DA treatment leads to cell death *in vitro* (Ben-Shachar et al., 2004; Cantuti-Castelvetri et al., 2003; Hastings et al., 1996; La Voie and Hastings, 1999; Masserano et al., 1996; Rabinovic et al., 2000; Xu et al., 2002; Zigmond et al., 2002). Moreover, although differing from classic Lewy bodies, dopamine-dependent neuronal inclusions have been experimentally generated in mice and cultured cells treated with METH (Fornai et al., 2004). The fact that various antioxidants can prevent DA neurotoxicity suggests oxidative stress occurring during DA metabolism might damage crucial neuronal functions and reduce survival. Indeed, the aging of human brain, which is an important risk factor for PD, is closely associated with attenuated antioxidant pathways challenged by oxidative stress (Lee et al., 2000; Lu et al., 2004). Considering constitutively high DA levels might expose DA neurons to chronic oxidative stress, one can assume Pael-R Tg mice are more sensitive than WT littermates to DA neurotoxins. DA neurotoxins such as MPTP and 6-OHDA are thought to disturb the mitochondrial activity of DA neurons possibly by promoting leakage of electrons from the mitochondrial electron transfer system and thereby generating reactive oxygen species. The levels of DAT and VMAT2 are reported to determine the sensitivity of neurons to DA neurotoxins. However, the resistance of Pael-R KO mice to MPTP was not explained by cell-surface levels of DAT in the striatum, which was shown to be significantly increased in Pael-R KO mice (Marazziti et al., 2007). The examination of cell-surface DAT level of Pael-R Tg mice, therefore, will be important to elucidate whether their sensitivity to DA neurotoxins is based on DAT-dependent mechanisms involving dysregulation of DA metabolism in the future.

Our results from Pael-R mutant mice strongly suggest that the Pael-R signal regulates the amount of DA in the dopaminergic neurons and that excessive Pael-R expression renders dopaminergic neurons susceptible to chronic DA toxicity. Further analysis of Pael-R mutant mice could provide useful information on the nigrostriatal DA metabolism and therapeutic strategy of PD.

Acknowledgments

The authors would like to thank Nagatsu T. and Sawada M. for helpful discussion, Meiji Institute of Health Science for MS12, Miyazaki J.-I. for pCAGGS-Cre, Yagi T. for pDT-ApA, the Research Resource Center of the Brain Science Institute for embryo manipulation and support for these animal experiments. This work was partially supported by the Ministry of Education, Science, Sports and Culture, Grant-in-Aid for Scientific Research on Priority Areas – Advanced Brain Science Project – #15016120 to R.T., for Scientific Research (A) #14207032 to R.T., and for Young Scientists (A) #15680011 to Y.I. and a grant from the Special Postdoctoral Researcher Program of RIKEN to Y.I.

References

Bamford, N.S., Zhang, H., Schmitz, Y., Wu, N.P., Cepeda, C., Levine, M.S., Schmauss, C., Zakharenko, S.S., Zablow, L., Sulzer, D., 2004. Heterosy-

naptic dopamine neurotransmission selects sets of corticostriatal terminals. Neuron 42, 653–663.

Ben-Shachar, D., Zuk, R., Gazawi, H., Ljubuncic, P., 2004. Dopamine toxicity involves mitochondrial complex I inhibition: implications to dopamine-related neuropsychiatric disorders. Biochem. Pharmacol. 67, 1965–1974.

Betarbet, R., Sherer, T.B., Greenamyre, J.T., 2002. Animal models of Parkinson's disease. Bioessays 24, 308–318.

Borchelt, D.R., Davis, J., Fischer, M., Lee, M.K., Slunt, H.H., Ratovitsky, T., Regard, J., Copeland, N.G., Jenkins, N.A., Sisodia, S.S., Price, D.L., 1996. A vector for expressing foreign genes in the brains and hearts of transgenic mice. Genet. Anal. 13, 159–163.

Calabresi, P., Fedele, E., Pisani, A., Fontana, G., Mercuri, N.B., Bernardi, G., Raiteri, M., 1995. Transmitter release associated with long-term synaptic depression in rat corticostriatal slices. Eur. J. Neurosci. 7, 1889–1894.

Cantuti-Castelvetri, I., Shukitt-Hale, B., Joseph, J.A., 2003. Dopamine neurotoxicity: age-dependent behavioral and histological effects. Neurobiol. Aging 24, 697–706.

Centonze, D., Picconi, B., Baunez, C., Borrelli, E., Pisani, A., Bernardi, G., Calabresi, P., 2002. Cocaine and amphetamine depress striatal GABAergic synaptic transmission through D2 dopamine receptors. Neuropsychopharmacology 26, 164–175.

Centonze, D., Grande, C., Usiello, A., Gubellini, P., Erbs, E., Martin, A.B., Pisani, A., Tognazzi, N., Bernardi, G., Moratalla, R., Borrelli, E., Calabresi, P., 2003. Receptor subtypes involved in the presynaptic and postsynaptic actions of dopamine on striatal interneurons. J. Neurosci. 23, 6245–6254.

Centonze, D., Gubellini, P., Usiello, A., Rossi, S., Tscherter, A., Bracci, E., Erbs, E., Tognazzi, N., Bernardi, G., Pisani, A., Calabresi, P., Borrelli, E., 2004. Differential contribution of dopamine D2S and D2L receptors in the modulation of glutamate and GABA transmission in the striatum. Neuroscience 129, 157–166.

Chui, D.H., Tanahashi, H., Ozawa, K., Ikeda, S., Checler, F., Ueda, O., Suzuki, H., Araki, W., Inoue, H., Shirotani, K., Takahashi, K., Gallyas, F., Tabira, T., 1999. Transgenic mice with Alzheimer presenilin 1 mutations show accelerated neurodegeneration without amyloid plaque formation. Nat. Med. 5, 560–564.

Donohue, P.J., Shapira, H., Mantey, S.A., Hampton, L.L., Jensen, R.T., Battey, J.F., 1998. A human gene encodes a putative G protein-coupled receptor highly expressed in the central nervous system. Brain Res. Mol. Brain Res. 54, 152–160.

Fornai, F., Lenzi, P., Gesi, M., Soldani, P., Ferrucci, M., Lazzeri, G., Capobianco, L., Battaglia, G., De Blasi, A., Nicoletti, F., Paparelli, A., 2004. Methamphetamine produces neuronal inclusions in the nigrostriatal system and in PC12 cells. J. Neurochem. 88, 114–123.

Fumagalli, F., Gainetdinov, R.R., Valenzano, K.J., Caron, M.G., 1998. Role of dopamine transporter in methamphetamine-induced neurotoxicity: evidence from mice lacking the transporter. J. Neurosci. 18, 4861–4869.

Goldberg, M.S., Fleming, S.M., Palacino, J.J., Cepeda, C., Lam, H.A., Bhatnagar, A., Meloni, E.G., Wu, N., Ackerson, L.C., Klapstein, G.J., Gajendiran, M., Roth, B.L., Chesselet, M.F., Maidment, N.T., Levine, M.S., Shen, J., 2003. Parkin-deficient mice exhibit nigrostriatal deficits but not loss of dopaminergic neurons. J. Biol. Chem. 278, 43628–43635.

Gomi, H., Yokoyama, T., Fujimoto, K., Ikeda, T., Katoh, A., Itoh, T., Itohara, S., 1995. Mice devoid of the glial fibrillary acidic protein develop normally and are susceptible to scrapie prions. Neuron 14, 29–41.

Hastings, T.G., Lewis, D.A., Zigmond, M.J., 1996. Role of oxidation in the neurotoxic effects of intrastriatal dopamine injections. Proc. Natl. Acad. Sci. U.S.A. 93, 1956–1961.

Imai, Y., Soda, M., Takahashi, R., 2000. Parkin suppresses unfolded protein stress-induced cell death through its E3 ubiquitin–protein ligase activity. J. Biol. Chem. 275, 35661–35664.

Imai, Y., Soda, M., Inoue, H., Hattori, N., Mizuno, Y., Takahashi, R., 2001. An unfolded putative transmembrane polypeptide, which can lead to endoplasmic reticulum stress, is a substrate of Parkin. Cell 105, 891–902.

Imai, Y., Soda, M., Hatakeyama, S., Akagi, T., Hashikawa, T., Nakayama, K.I., Takahashi, R., 2002. CHIP is associated with Parkin, a gene responsible for familial Parkinson's disease, and enhances its ubiquitin ligase activity. Mol. Cell. 10, 55–67.

Itier, J.M., Ibanez, P., Mena, M.A., Abbas, N., Cohen-Salmon, C., Bohme, G.A., Laville, M., Pratt, J., Corti, O., Pradier, L., Ret, G., Joubert, C., Periquet, M., Araujo, F., Negroni, J., Casarejos, M.J., Canals, S., Solano, R., Serrano, A., Gallego, E., Sanchez, M., Denefle, P., Benavides, J., Tremp, G., Rooney, T.A., Brice, A., Garcia de Yebenes, J., 2003. Parkin gene inactivation alters behaviour and dopamine neurotransmission in the mouse. Hum. Mol. Genet. 12, 2277–2291.

Ito, S., Kato, T., Fujita, K., 1988. Covalent binding of catechols to proteins through the sulphydryl group. Biochem. Pharmacol. 37, 1707–1710.

Kaneko, S., Hikida, T., Watanabe, D., Ichinose, H., Nagatsu, T., Kreitman, R.J., Pastan, I., Nakanishi, S., 2000. Synaptic integration mediated by striatal cholinergic interneurons in basal ganglia function. Science 289, 633–637.

Kawasawa, Y., McKenzie, L.M., Hill, D.P., Bono, H., Yanagisawa, M., 2003. G protein-coupled receptor genes in the FANTOM2 database. Genome Res. 13, 1466–1477.

Kitada, T., Asakawa, S., Hattori, N., Matsumine, H., Yamamura, Y., Minoshima, S., Yokochi, M., Mizuno, Y., Shimizu, N., 1998. Mutations in the parkin gene cause autosomal recessive juvenile parkinsonism. Nature 392, 605–608.

LaVoie, M.J., Hastings, T.G., 1999. Dopamine quinone formation and protein modification associated with the striatal neurotoxicity of methamphetamine: evidence against a role for extracellular dopamine. J. Neurosci. 19, 1484–1491.

Lee, C.K., Weindruch, R., Prolla, T.A., 2000. Gene-expression profile of the ageing brain in mice. Nat. Genet. 25, 294–297.

Lu, T., Pan, Y., Kao, S.Y., Li, C., Kohane, I., Chan, J., Yankner, B.A., 2004. Gene regulation and DNA damage in the ageing human brain. Nature 429, 883–891.

Marazziti, D., Gallo, A., Golini, E., Matteoni, R., Tocchini-Valentini, G.P., 1998. Molecular cloning and chromosomal localization of the mouse Gpr37 gene encoding an orphan G-protein-coupled peptide receptor expressed in brain and testis. Genomics 53, 315–324.

Marazziti, D., Golini, E., Mandillo, S., Magrelli, A., Witke, W., Matteoni, R., Tocchini-Valentini, G.P., 2004. Altered dopamine signaling and MPTP resistance in mice lacking the Parkinson's disease-associated GPR37/parkin-associated endothelin-like receptor. Proc. Natl. Acad. Sci. U.S.A. 101, 10189–10194.

Marazziti, D., Mandillo, S., Di Pietro, C., Golini, E., Matteoni, R., Tocchini-Valentini, G.P., 2007. GPR37 associates with the dopamine transporter to modulate dopamine uptake and behavioral responses to dopaminergic drugs. Proc. Natl. Acad. Sci. U.S.A. 104, 9846–9851.

Masserano, J.M., Gong, L., Kulaga, H., Baker, I., Wyatt, R.J., 1996. Dopamine induces apoptotic cell death of a catecholaminergic cell line derived from the central nervous system. Mol. Pharmacol. 50, 1309–1315.

Murakami, T., Shoji, M., Imai, Y., Inoue, H., Kawarabayashi, T., Matsubara, E., Harigaya, Y., Sasaki, A., Takahashi, R., Abe, K., 2004. Pael-R is accumulated in Lewy bodies of Parkinson's disease. Ann. Neurol. 55, 439–442.

Nelson, E.L., Liang, C.L., Sinton, C.M., German, D.C., 1996. Midbrain dopaminergic neurons in the mouse: computer-assisted mapping. J. Comp. Neurol. 369, 361–371.

Rabinovic, A.D., Lewis, D.A., Hastings, T.G., 2000. Role of oxidative changes in the degeneration of dopamine terminals after injection of neurotoxic levels of dopamine. Neuroscience 101, 67–76.

Rezgaoui, M., Susens, U., Ignatov, A., Gelderblom, M., Glassmeier, G., Franke, I., Urny, J., Imai, Y., Takahashi, R., Schaller, H.C., 2006. The neuropeptide head activator is a high-affinity ligand for the orphan G-protein-coupled receptor GPR37. J. Cell. Sci. 119, 542–549.

Shimura, H., Hattori, N., Kubo, S., Mizuno, Y., Asakawa, S., Minoshima, S., Shimizu, N., Iwai, K., Chiba, T., Tanaka, K., Suzuki, T., 2000. Familial Parkinson disease gene product, parkin, is a ubiquitin–protein ligase. Nat. Genet. 25, 302–305.

Sunaga, S., Maki, K., Komagata, Y., Ikuta, K., Miyazaki, J.I., 1997. Efficient removal of loxP-flanked DNA sequences in a gene-targeted locus by transient expression of Cre recombinase in fertilized eggs. Mol. Reprod. Dev. 46, 109–113.

Tateno, M., Sadakata, H., Tanaka, M., Itohara, S., Shin, R.M., Miura, M., Masuda, M., Aosaki, T., Urushitani, M., Misawa, H., Takahashi, R., 2004. Calcium-permeable AMPA receptors promote misfolding of mutant SOD1 protein and development of amyotrophic lateral sclerosis in a transgenic mouse model. Hum. Mol. Genet. 13, 2183–2196.

Valdenaire, O., Giller, T., Breu, V., Ardati, A., Schweizer, A., Richards, J.G., 1998. A new family of orphan G protein-coupled receptors predominantly expressed in the brain. FEBS Lett. 424, 193–196.

West, M.J., 1999. Stereological methods for estimating the total number of neurons and synapses: issues of precision and bias. Trends Neurosci. 22, 51–61.

Wieczorek, W.J., Kruk, Z.L., 1994. A quantitative comparison on the effects of benztropine, cocaine and nomifensine on electrically evoked dopamine overflow and rate of re-uptake in the caudate putamen and nucleus accumbens in the rat brain slice. Brain Res. 657, 42–50.

Xu, J., Kao, S.Y., Lee, F.J., Song, W., Jin, L.W., Yankner, B.A., 2002. Dopamine-dependent neurotoxicity of alpha-synuclein: a mechanism for selective neurodegeneration in Parkinson disease. Nat. Med. 8, 600–606.

Yanagawa, Y., Kobayashi, T., Ohnishi, M., Tamura, S., Tsuzuki, T., Sanbo, M., Yagi, T., Tashiro, F., Miyazaki, J., 1999. Enrichment and efficient screening of ES cells containing a targeted mutation: the use of DT-A gene with the polyadenylation signal as a negative selection maker. Transgenic Res. 8, 215–221.

Yang, Y., Nishimura, I., Imai, Y., Takahashi, R., Lu, B., 2003. Parkin suppresses dopaminergic neuron-selective neurotoxicity induced by Pael-R in *Drosophila*. Neuron 37, 911–924.

Zhang, Y., Gao, J., Chung, K.K., Huang, H., Dawson, V.L., Dawson, T.M., 2000. Parkin functions as an E2-dependent ubiquitin–protein ligase and promotes the degradation of the synaptic vesicle-associated protein, CDCrel-1. Proc. Natl. Acad. Sci. U.S.A. 97, 13354–13359.

Zhou, Q.Y., Palmiter, R.D., 1995. Dopamine-deficient mice are severely hypoactive, adipsic, and aphagic. Cell 83, 1197–1209.

Zigmond, M.J., Hastings, T.G., Perez, R.G., 2002. Increased dopamine turnover after partial loss of dopaminergic neurons: compensation or toxicity? Parkinsonism Relat. Disord. 8, 389–393.

パーキンソン病の成因

竹内　啓喜　　高橋　良輔

日本老年医学会雑誌　第44巻　第4号　別刷

老年医学の展望

パーキンソン病の成因

竹内　啓喜　　高橋　良輔

要　約　これまでの多くの研究により，パーキンソン病の原因に関して様々な仮説が提唱され，多くのことがわかってきた．その全貌については今なお不明な点も多いが，環境要因と遺伝要因の複合により発症すると考えられている．環境要因については加齢，また農薬や神経伝達物質であるドーパミンが酸化して生じるキノン類等による酸化ストレスの増大，遺伝要因ではミトコンドリア機能に関わるタンパク質や，不要となったり産生の際に異常を来したりしたタンパク質の分解経路，とくにユビキチン—プロテアソーム系の機能不全によるα-シヌクレイン（α-synuclein）の凝集が注目されている．本稿ではこれまでに明らかになったパーキンソン病の発症に関わっていると思われるメカニズムについて，環境要因と遺伝要因それぞれについてまとめた．

Key words：パーキンソン病，農薬，酸化ストレス，α-シヌクレイン，ユビキチン—プロテアソーム系

（日老医誌　2007；44：415–421）

はじめに

パーキンソン病（PD）は，安静時振戦，筋固縮，寡動，姿勢反射障害を4大徴候とする神経変性疾患である．これらの神経学的徴候は中脳黒質のドーパミン作動性神経細胞死によるドーパミン量の低下が直接の原因であり，病理学的にはレビー小体という細胞内封入体を特徴とする．しかし細胞死の原因やレビー小体の成因については，これまでの様々な研究から多くのことが明らかになってきているものの，その全体像については未だ不明である．一般的には，孤発性PDは何らかの遺伝要因と環境要因とが重なってミトコンドリアの機能障害や炎症反応による酸化ストレスの増大，また不要タンパク質の分解処理能が低下して蓄積して生じる細胞毒性でドーパミン作動性神経が細胞死を起こして発症するとされているが，そのメカニズムについては議論が分かれている．そこで孤発性PDと，その研究を大きく前進させることになった家族性PDについてこれまでに示されてきたことを元に，現在考えられているPDの成因についてまとめた．

環境要因

孤発性PDの原因については，これまでの疫学調査で多くのものが候補として挙げられてきた．代表的なものとしては加齢と農薬への曝露で[1]，加齢についてはATP依存性タンパク質分解経路であるユビキチン—プロテアソーム系の機能低下が想定されている[2]．農薬については，農村部での居住，井戸水の利用，農作業への従事がPDのリスクとなっている[3]ことより疑われる一方，PDとよく似た症状をおこす物質が発見されて一部はPDの疾患モデル作製に応用された[4]（表1）．これらは酸化ストレスを増大させることでドーパミン作動性神経に選択的に細胞死を起こし，直接活性酸素種（Reactive oxygen species; ROS）を産生するディルドリン[5]（本邦では製造中止），ミトコンドリア電子伝達系阻害によるものとしてはパラコート，ロテノンなどがある．除草剤として使われるパラコートは可逆的ではあるが，マウス中脳黒質ドーパミン神経内でレビー小体の主要構成成分であるα-synucleinの集簇を促す[6]．ロテノンはマメ科植物の根から得られる天然由来の農薬であるが，慢性投与によりミトコンドリア電子伝達系複合体Iを阻害しラットにPDと似た症状を示すだけでなく黒質から線条体にかけてのドーパミン神経の減少と細胞質内にレビー小体に似た封入体が形成する[7]．これまでの薬物モデルでは封入体形成がみられないことを考えると，ロテノンはPDの病態に近いモデルを作製できる毒物として有用なものと思われる．また農薬とは別にPDモデル作製に使われているものとしてMPTP，6-ヒドロキシドーパミン（6-OHDA）などがある．いずれもドーパミントランスポー

H. Takeuchi, R. Takahashi：京都大学大学院医学研究科臨床神経学（神経内科）

表1　パーキンソン病関連因子とモデル作製に使う毒物

正の相関	モデル作製に使う毒物	負の相関
加齢	6-OHDA	喫煙（ニコチン？）
農村部での居住	MPTP	コーヒー（カフェイン？）
井戸水の使用	ロテノン	
農業への従事	パラコート	
農薬への曝露	ディルドリン（本邦では使用中止）	

ターによってドーパミン神経に取り込まれることで選択毒性を発揮し，ミトコンドリア電子伝達系複合体Iを阻害し，ROSの産生を上昇させて毒性を発揮する．MPTPは麻薬中毒患者にPD様症状がみられたのをきっかけに合成麻薬の不純物として発見され[8]，PD研究を飛躍させることになった．また，以前より毒物モデル作製に用いられている6-OHDAはドーパミンの水酸化物として得られたものであるが内因性に存在し，ドーパミン神経を傷害する可能性が示唆されている[9]．既に知られている内因性のドーパミン神経毒性を持つ物質としてはドーパミンの自己酸化により生成されるイソキノリン類[10]や，β-カルボリン誘導体[11][12]が知られる．いずれにせよこれらPDとよく似た特徴を示す薬物は，概して酸化ストレス増大を引き起こすものである．なお金属イオン中毒もマンガンを主体に取り上げられているが，既に発症しているPDを悪化させるものの，一次的な原因としての根拠は不十分である[13]．プロテアソーム阻害薬でPDモデル動物を作製したとの報告もあるが[14]，この結果は再現性に問題があることが指摘されている[15][16]．また，逆に保護的であったとの報告もあり[17]，統一した見解は得られていない．

一方，PDと負の相関を持つ因子も調査されており，代表的なものとして喫煙[18]とコーヒー摂取[19]があげられている．いずれもそのメカニズムについてはよくわかっていないが，喫煙については，ニコチンの作用が挙げられており，ニコチン受容体を介して黒質のドーパミン神経からのドーパミン遊離を促す[20]，神経保護効果としてはPI3K-Aktシグナル伝達によりBcl familyを活性化する[21]，あるいはNF-κB抑制によりアポトーシスを抑制する[22]，free radical scavenger作用をもち酸化ストレスを直接減少させる[23]，ミクログリアからの細胞傷害因子放出を抑制する[24]，などが報告されている．またコーヒーは，カフェインがアデノシンA_{2A}受容体を阻害することにより細胞保護効果を示していると考えられている[25]．これらの臨床応用はそのままでは依存性や忍容性，他臓器への影響の面で問題があるため，コリンエステラーゼ阻害薬やニコチン受容体のアゴニスト，他のアデノシンA_{2A}受容体阻害薬の使用が期待される．また，NSAIDsが神経細胞脱落部位での炎症反応を抑制することで神経保護に働くと考えられたが，疫学調査では効果は部分的なようである[26]．

遺伝要因

1．家族性PD

PDは90%が明らかな家族歴のない孤発性で，家族性（即ち遺伝性）のものは5～10%程度と少ない[27]．しかし家族性症例の原因遺伝子を突き止めることが孤発例の原因解明につながるため，PDでも同様に家族例について多くの研究がなされ，その結果PDの発症メカニズムについて多くのことがわかってきた．以下，これまでに原因遺伝子が明らかになった家族性PDとその遺伝子について述べる．主だった特徴については別表にまとめた（表2）．

A．常染色体優性遺伝

PARK1，PARK4はα-synuclein遺伝子の変異による．表現型は孤発性PDとほぼ同じでL-ドーパも有効だが，発症年齢が40～50代と若年傾向で認知症が目立つ．病理学的所見も孤発性PDと似通っているが，レビー小体が黒質だけでなく皮質でもみられる．これまでに知られている変異は53番目のアラニンがスレオニンに，30番目のアラニンがプロリンに，46番目のグルタミン酸がリジンに（A53T，A30P，E46K）[28]～[30]変異したものであり，これらは正常型より凝集しやすい．α-synucleinの生理機能はシナプス前に存在し，ドーパミン放出や再取り込みにかかわるはたらきを持つことが報告され[31][32]，α-synucleinの機能不全が神経毒性をもつドーパミンの自己酸化生成物を増大させることでドーパミン神経細胞死が生じるのかもしれない[33]．

PARK1の報告例は少ないが，レビー小体の主要成分がユビキチン化やリン酸化を受けたα-synucleinであることが明らかになり，注目を集めるようになった[34]～[36]．α-synucleinが何らかの理由により凝集して細胞毒性を発揮し，ドーパミン神経に選択的に細胞死をおこす，という孤発性PDの発症仮説のもと，様々な遺伝子改変動物がつくられている．ヒト正常型α-synucleinや前述の変異α-synucleinを導入したショウジョウバエではドーパミン作動性神経の減少，レビー小体様の細胞内封入体やα-synucleinのフィブリルが形成され，運動機能障害の表現型がみられるが[37]，マウスでは細胞内封入体やフィブリル形成が見られてもドーパミン作動性神経の脱